July 1, 1965

George C. Marshall Space Flight Center
Huntsville, Alabama

BUREAU OF ENGINEERING RESEARCH

MUTUAL IMPEDANCE EFFECTS IN SCANNED ANTENNA ARRAYS

Technical Report No. 2
Contract NAS8-11295

by

Dr. Harold Mott
Professor of Electrical Engineering
Project Director

and

David N. McQuiddy

BER

COLLEGE OF ENGINEERING

THE UNIVERSITY OF ALABAMA 1831

UNIVERSITY OF ALABAMA

UNIVERSITY ALABAMA

University of Alabama
Bureau of Engineering Research
University, Alabama

MUTUAL IMPEDANCE EFFECTS IN SCANNED ANTENNA ARRAYS

Technical Report No. 2
Contract NAS8-11295
July 1, 1965

by

Dr. Harold Mott
Professor of Electrical Engineering
Project Director

and

David N. McQuiddy

Prepared for

George C. Marshall Space Flight Center
Huntsville, Alabama

TABLE OF CONTENTS

LIST OF ILLUSTRATIONS

ACKNOWLEDGEMENT

This report has been prepared for the Instrumentation Branch, Astrionics Division, George C. Marshall Space Flight Center, Huntsville, Alabama, under Contract NAS8-11295.

The authors wish to express their appreciation to Mr. Donald Stone and Mr. Paul Swindall of the Astrionics Division for their helpful advice and discussions. Appreciation is also expressed to Mr. J. W. Harper of the Astrionics Division for his interest and valuable help. The authors wish also to acknowledge the administrative assistance of Professor L. A. Woodman, Director, Bureau of Engineering Research.

ABSTRACT

The results of a study of the current literature dealing with mutual impedance effects in electronically-scanned antenna arrays are presented.

Various methods of minimizing the harmful effects of impedance variation with scan angle are analyzed.

Factors contributing to the optimum design of arrays are presented.

author

I. INTRODUCTION

When the beam direction of a scanned antenna array is changed by varying the phase and amplitude of the currents in the array elements mutual coupling of the elements causes the driving-point impedances to vary. This may be seen from the loop equations describing the system,

$$\begin{aligned} V_1 &= Z_{11}I_1 + Z_{12}I_2 + Z_{13}I_3 + \ldots + Z_{1N}I_N \\ V_2 &= Z_{21}I_1 + Z_{22}I_2 + Z_{23}I_3 + \ldots + Z_{2N}I_N \\ &\ldots\ldots\ldots\ldots\ldots\ldots\ldots \\ V_N &= Z_{N1}I_1 + Z_{N2}I_2 + Z_{N3}I_3 + \ldots + Z_{NN}I_N \end{aligned} \tag{1}$$

The driving-point impedance of any element, e.g. element 1, is the ratio of applied voltage to input current

$$Z_1 = \frac{V_1}{I_1} = Z_{11} + \frac{I_2}{I_1} Z_{12} + \frac{I_3}{I_1} Z_{13} + \ldots + \frac{I_N}{I_1} Z_{1N} \tag{2}$$

It is clear from Eq. (2) that the input impedance depends on the amplitude and phases of currents in all array elements, even though the mutual impedances between the elements are constant.

This mutual coupling between array elements has several undesired effects. Even for non-scanned arrays the coupling changes the driving-point impedance of each element from a value calculated or measured for the isolated element; furthermore for finite arrays the impedance becomes a function of element position.

As the array is scanned the variation in driving point impedances may cause the transmitter to transfer power to the antenna less efficiently because of impedance mismatch, decreasing the system gain. In a large array relatively few elements are near an edge of the array and the input

impedances of most of the elements are substantially identical. Then the identical variation of impedances does not by itself change the radiation pattern. For smaller arrays, however, the influence of elements near the edge is more important, and the impedances of these elements do not change with scan angle in the same way as for the center elements. This non-uniform change in input impedances may cause pattern distortion, because of the non-uniform change in element currents.

Cases have been observed in which the resistive component of the driving-point impedance of an element near the edge has become negative, causing this element to absorb power from the rest of the array.[1] Such wide variation in impedance can of course easily cause generators to become unstable unless protected by isolators.

This report will discuss these problems in more detail. The mutual impedance effects in arrays of typical elements will be described quantitatively. Finally, procedures which will help to lessen these problems will be given.

II. MUTUAL IMPEDANCE BETWEEN ARRAY ELEMENTS

The Induced EMF Method

The EMF method developed by Carter[2] has been the most widely used procedure for determining mutual impedance between linear array elements. Using Carson's reciprocity theorem[3,4] he developed equations for the self impedance of an isolated element and the mutual impedance between pairs of elements.[5]

$$Z_{11} = \frac{-1}{I_1^2(o)} \int_o^{L_1} E_{11} I_1(s)\, ds \tag{3}$$

$$Z_{21} = - \frac{1}{I_1(o) I_2(o)} \int_o^{L_2} E_{21}(s)\, I_2(s)\, ds \tag{4}$$

where $I_1(o)$ is the input current to antenna 1 when antenna 2 is floating, E_{11} is the tangential field induced at the surface of antenna 1 by the current in antenna 1 (not the total field which is of course zero along a perfect conductor but only that portion caused by the current flow acting as an infinite impedance source), and $I_1(s)$ is the current distribution along the antenna when driven by a generator. For the mutual impedance equation, $I_1(o)$ is again the input current to antenna 1 when antenna 2 is floating. $I_2(o)$ is the input current to antenna 2 (when antenna 1 is floating) which produces the current $I_2(s)$ in antenna 2, and $E_{21}(s)$ is the field induced along antenna 2 (at the surface of antenna 2 when the presence of the conductor of antenna 2 is ignored) by the action of the current in antenna 1.

Calculations of mutual impedance between electric dipole elements are common[2,5,6]. A short example of the method is given here. Consider two monopole antennas above ground with heights H_1 and H_2 (Fig. 1). The

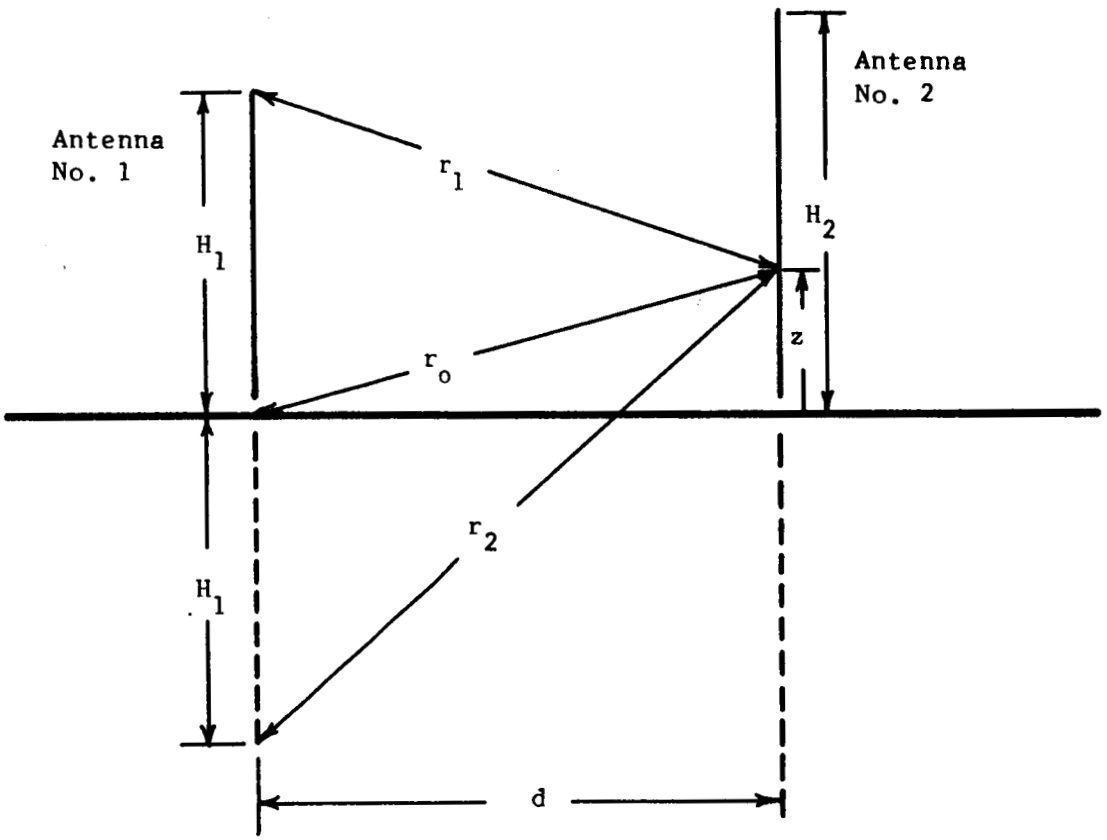

Fig. 1. Grounded Monopole Antennas

current in antenna 1 will be sinusoidal if the presence of antenna 2 is ignored, and vice versa

$$I_1(s) = I_{1m} \sin k (H_1 - z)$$
$$I_2(s) = I_{2m} \sin k (H_2 - z) \qquad (5)$$

The vertical component of the electric field at the position of antenna 2, produced by current in antenna 1, is[7]

$$E_{21} = 30 I_{1m} \left(- \frac{j\varepsilon^{-jkr_1}}{r_1} - \frac{j\varepsilon^{-jkr_2}}{r_2} + \frac{2j \cos k H_1 \varepsilon^{-jkr_o}}{r_o} \right) \qquad (6)$$

Substituting (6) into (4) gives

$$Z_{21} = - \frac{30 I_{1m} I_{2m}}{I_1(o) I_2(o)} \int_o^{H_2} \left[- \frac{j\varepsilon^{-jkr_1}}{r_1} - \frac{j\varepsilon^{-jkr_2}}{r_2} + \frac{2j \cos k H_1 \varepsilon^{-jkr_o}}{r_o} \right] \left[\sin k(H_2 - z) \right] dz \qquad (7)$$

It is common to refer the mutual impedance to current antinodes by setting

$$Z_{21}(\text{antinodes}) = Z_{21} \frac{I_1(o) I_2(o)}{I_{1m} I_{2m}} \qquad (8)$$

Doing so and carrying out the integration for antennas of equal height H gives

$$R_{21} = 30 \Big\langle \sin(kH) \cos(kH) \left[Si(u_2) - Si(v_2) - 2Si(v_1) + 2 Si(u_1) \right]$$
$$- \frac{\cos(2kH)}{2} \left[2Ci(u_1) - 2Ci(u_o) + 2Ci(v_1) - Ci(u_2) - Ci(v_2) \right]$$
$$- \left[Ci(u_1) - 2 Ci(u_o) + Ci(v_1) \right] \Big\rangle \qquad (9)$$

$$X_{21} = -30 \Big\langle \sin(kH)\cos(kH)\left[2Ci(v_1) - 2Ci(u_1) + Ci(v_2) - Ci(u_2)\right]$$

$$- \frac{\cos(2kH)}{2}\left[2Si(u_1) - 2Si(u_o) + 2Si(v_1) - Si(u_2) - Si(v_2)\right]$$

$$- \left[Si(u_1) - 2\,Si(u_o) + Si(v_1)\right]\Big\rangle \qquad (10)$$

where

$$u_o = kd$$

$$u_1 = k\left(\sqrt{d^2+H^2} - H\right) \qquad v_1 = k\left(\sqrt{d^2+H^2} + H\right)$$

$$u_2 = k\left(\sqrt{d^2+(2H)^2} + 2H\right) \qquad v_2 = k\left(\sqrt{d^2+(2H)^2} - 2H\right) \qquad (11)$$

$$Si(x) = \int_0^x \frac{\sin u}{u}\,du \qquad Ci(x) = -\int_x^\infty \frac{\cos u}{u}\,du$$

It is obvious that calculations of mutual impedance are not short. Fortunately, results are given in many places in the literature[2,5,6,8]. Some of the results are shown in Figs. 2 and 3.

An extension of this method to aperture elements by first obtaining equivalent magnetic current distributions for the aperture fields is straightforward. In fact the results obtained for dipole sources can be applied directly to apertures.

Carter, Jr. has extended the induced EMF method to the calculation of self and mutual impedances in electric dipole arrays driven by infinite impedance generators (current sources).[9] With this assumption about the generator the mutual impedance between two elements is independent of the presence of other elements.

To simplify calculations Carter considered the array shown in Fig. 4. The number of columns of dipole elements was taken as finite (61) and the number of rows infinite (array extended to infinity in the $\pm$ z directions).

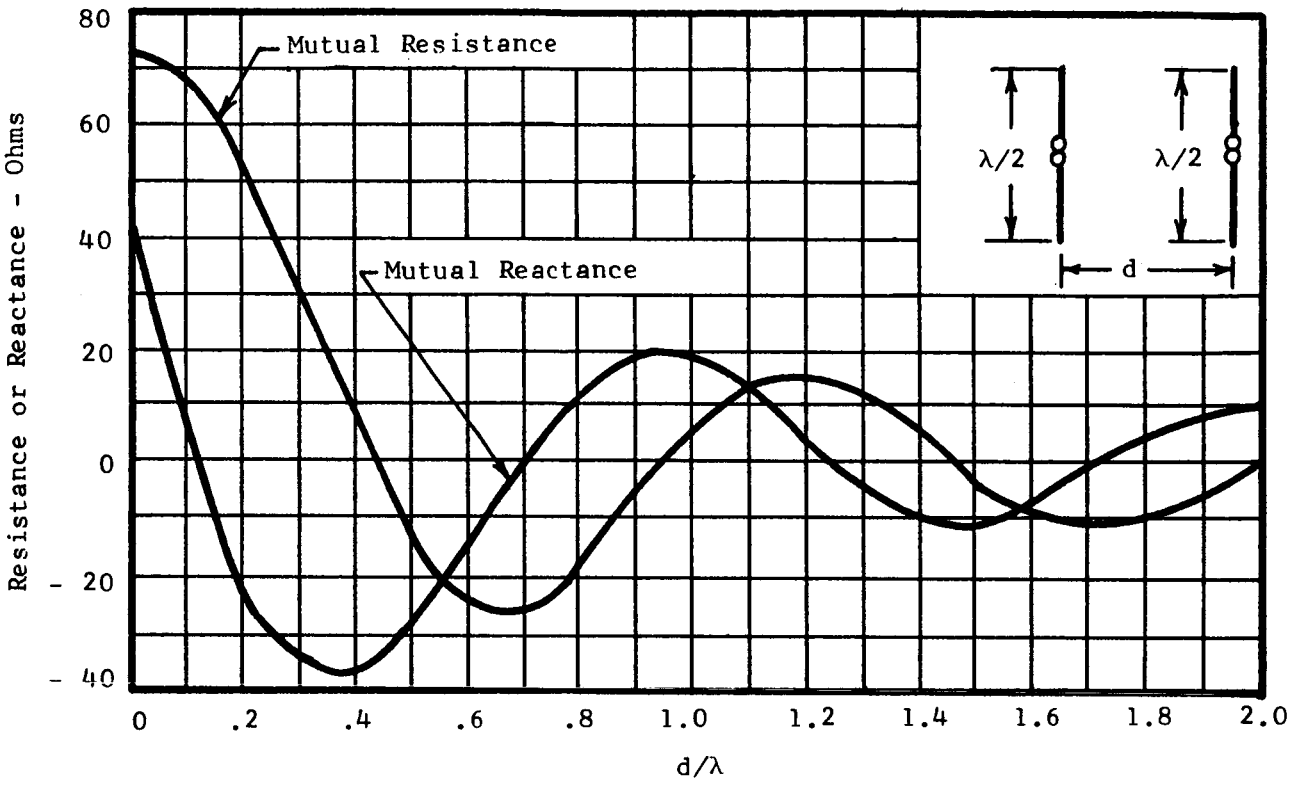

Fig. 2. Mutual Impedance between Parallel Half-Wave Antennas

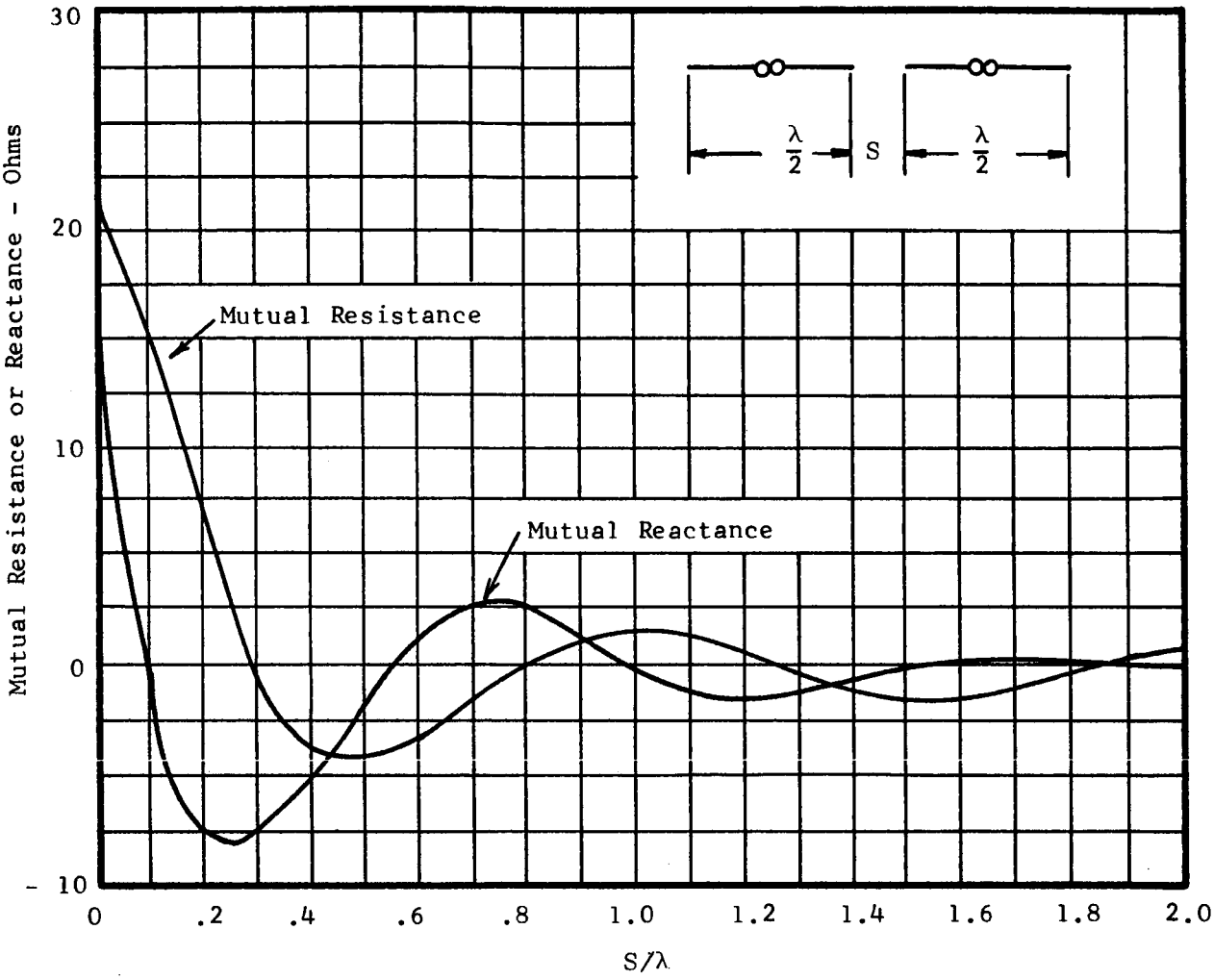

Fig. 3. Mutual Impedance between Collinear Half-Wave Antennas

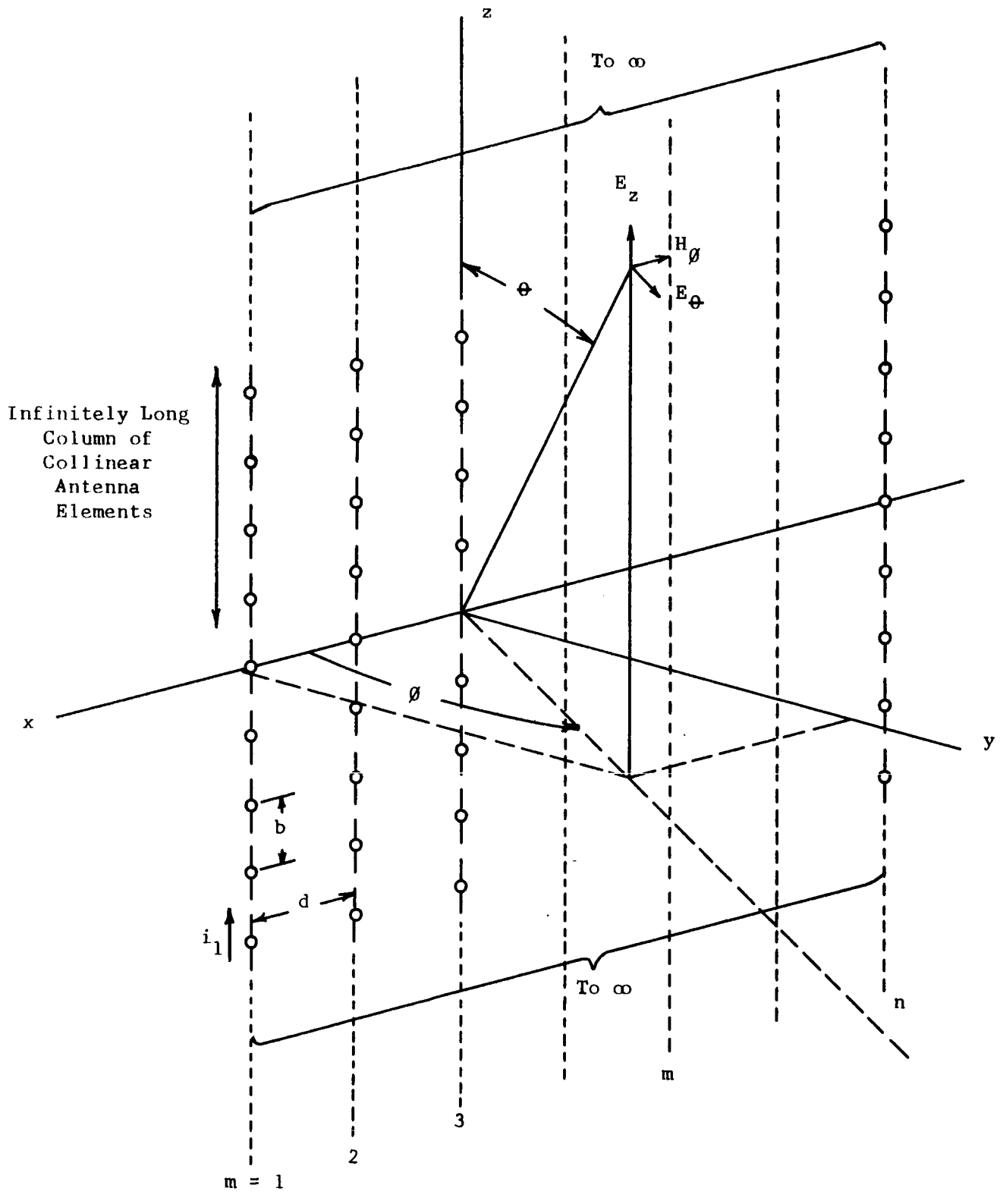

Fig. 4. Coordinates of Array

Each column of dipoles was treated as an infinitely long wire (instead of as discrete elements) with a current distribution on it corresponding to the current distribution that would exist if the dipoles were treated as discrete elements. This treatment is exact and not approximate, but it has the advantage that the fields from each wire can be found by wave functions in circular cylinder coordinates.[10] The computational procedure is long and complicated, and only some of Carter's results will be given here.

In the array of Fig. 1 the parameters chosen were dipole length = $\lambda/2$, b = $\lambda/2$ (corresponding to dipoles with ends touching), d = $\lambda/2$, radius of dipole element (necessary for calculating self reactance) = 0.005 λ. The current amplitudes at the center of the dipoles were uniform in the z direction but were tapered across the aperture according to

$$\left| I_p \right| = \left[0.33 + 0.67 \cos^2 \left(\frac{\frac{p}{2} - 15.5}{30.5} \pi \right) \right] I_o \qquad (12)$$

This is a symmetric function with a peak at the center element (element 31) and value at the edges of about one-third the peak value. According to Carter sidelobe levels for this taper are about 25 db below the main lobe maximum. The array was backed by a reflector at $\lambda/4$.

Two results are clear from Carter's work. The first is that driving-point impedances vary greatly according to element position in the array. The second is that the impedance of an element is a function of the scan angle.

Figure 5 gives the driving point impedances of elements 1 (at the edge of the array) through 31 (at the center) for broadside scan. The impedances do not differ greatly. Fig. 6 gives the impedances of the

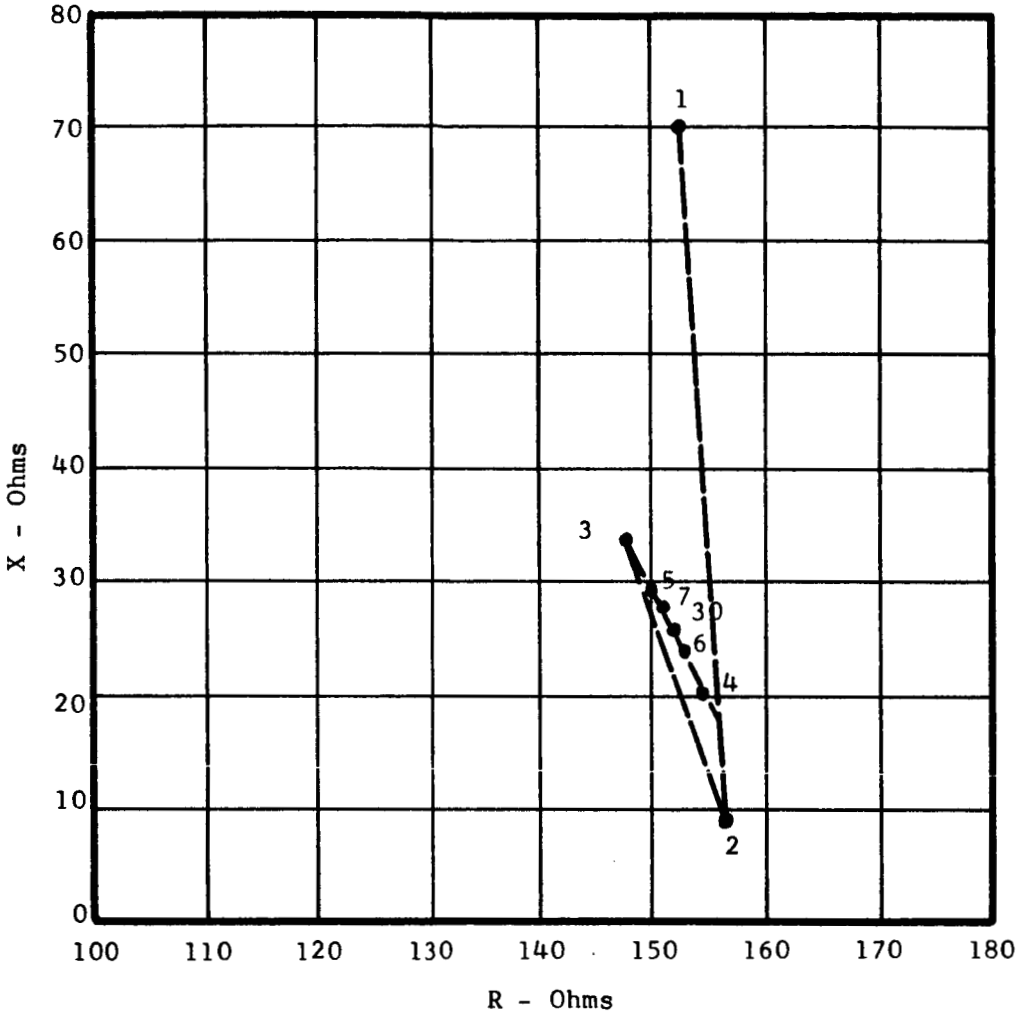

Fig. 5. Driving-Point Impedances of Half-Wave Dipole Array with Reflector, θ = 90°, ϕ = 90°

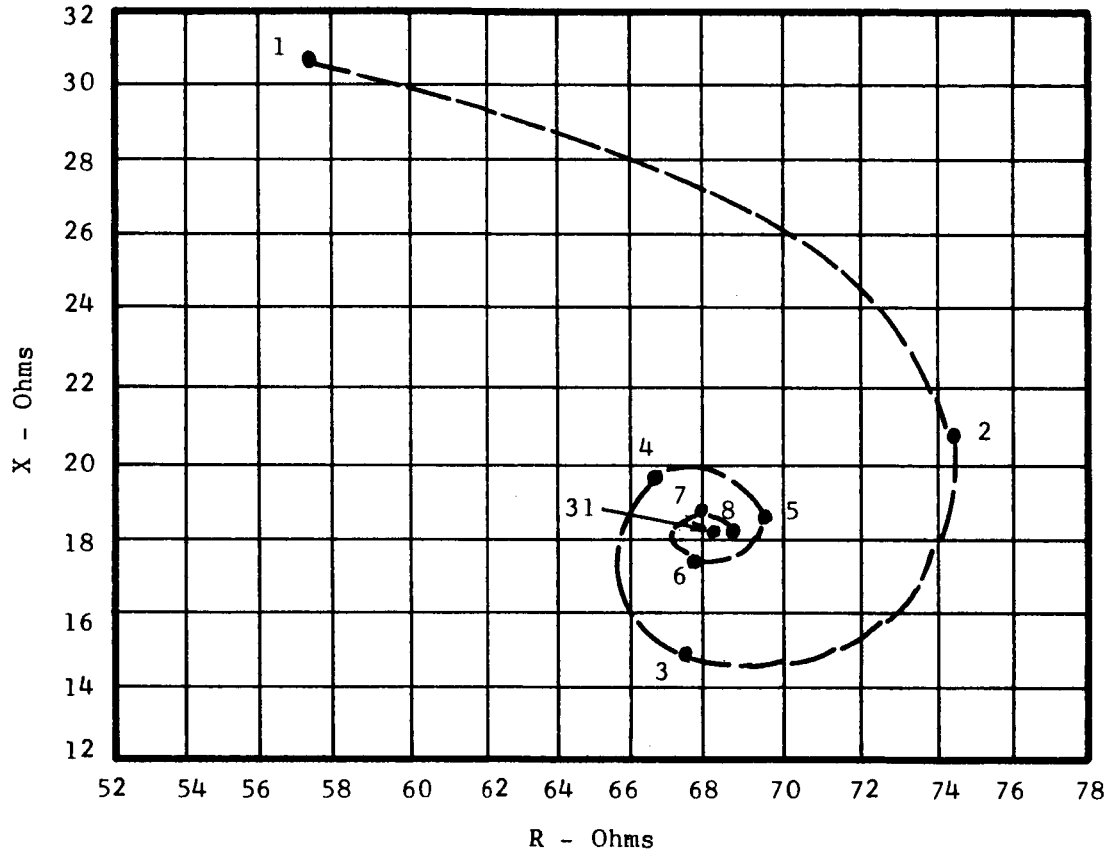

Fig. 6. Driving-Point Impedances of Half-Wave Dipole Array with Reflector, $\theta = 45°$, $\phi = 90°$

same elements for an E-plane scan angle of 45°. The impedances have changed considerably from their value at broadside, and now the variation between edge and center elements is much greater.

Figures 7 and 8 show the impedance of the center element (element 31) as a function of scan angles θ and ϕ through angles of 45° from broadside. If the generator for the center element is a lossless current source the change in radiated power is about -7.1 db for the E-plane scan $\theta = 45°$, $\phi = 90°$, about +1.07 db for the H-plane scan $\theta = 90°$, $\phi = 45°$, and about -9.7 db for the angles $\theta = 45°$, $\phi = 45°$.

Figure 9 is also taken from Carter's paper. It shows the impedance per unit length of the center wire of a grid of 61 wires with and without a reflector. Currents are equal in each wire. For an H-plane scan angle $\phi = 0°$ the change in radiated power from the center wire (from the broadside condition) is -11.5 db with reflector and +22.4 db without reflector.

A word of caution is necessary here. Carter's results apply only for the elements separately fed by current sources and the radiated power values given above are for such feeds. It follows then that an increase in driving-point resistance with scan angle leads to an increase in radiated power. In the more common case of dipoles fed by a voltage source this would not necessarily be true. Carter's results are quantitatively invalid for voltage sources, although his work is still valuable in indicating qualitatively the change in impedance with array position and scan angle. Carter points out that with his equations for mutual impedance the driving-point impedances for any assumed source impedances can be found, although he warns that this would be a large undertaking requiring the extensive use of a computer.

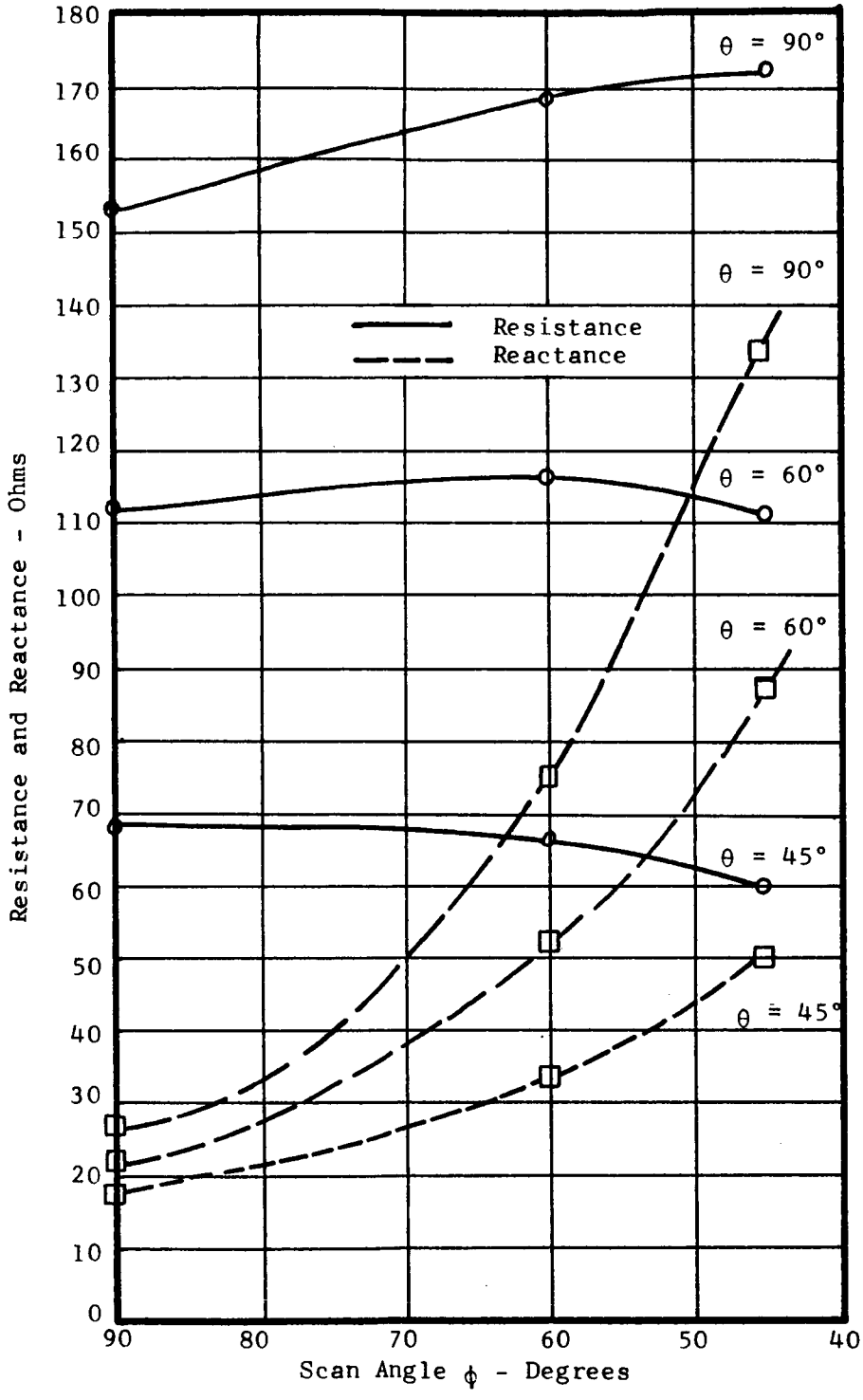

Fig. 7. Impedance vs Scan Angle of Element 31 of Half-Wave Dipole Array with Reflector, ϕ Scan

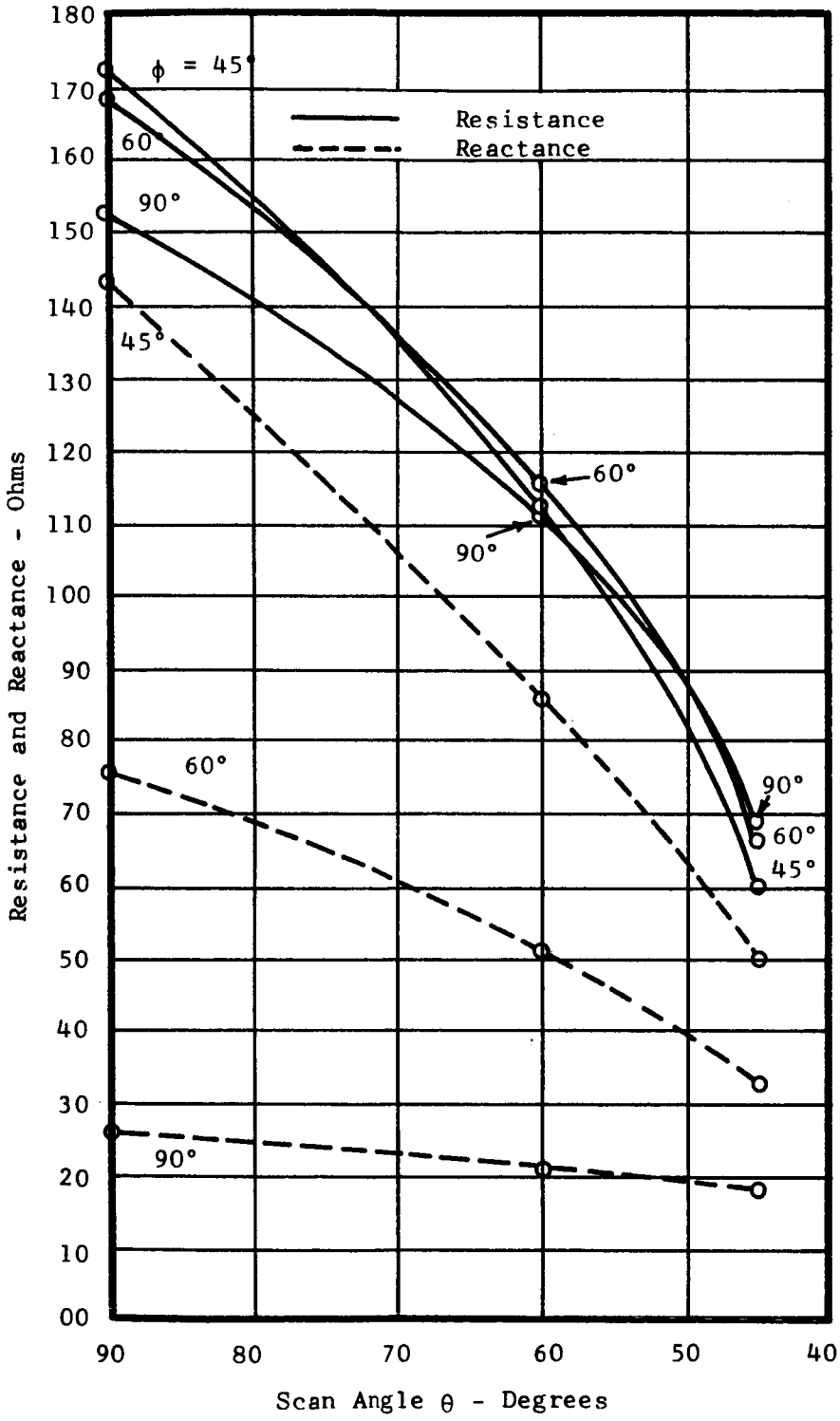

Fig. 8. Impedance vs Scan Angle of Element 31 of Half-Wave Dipole Array with Reflector, θ Scan

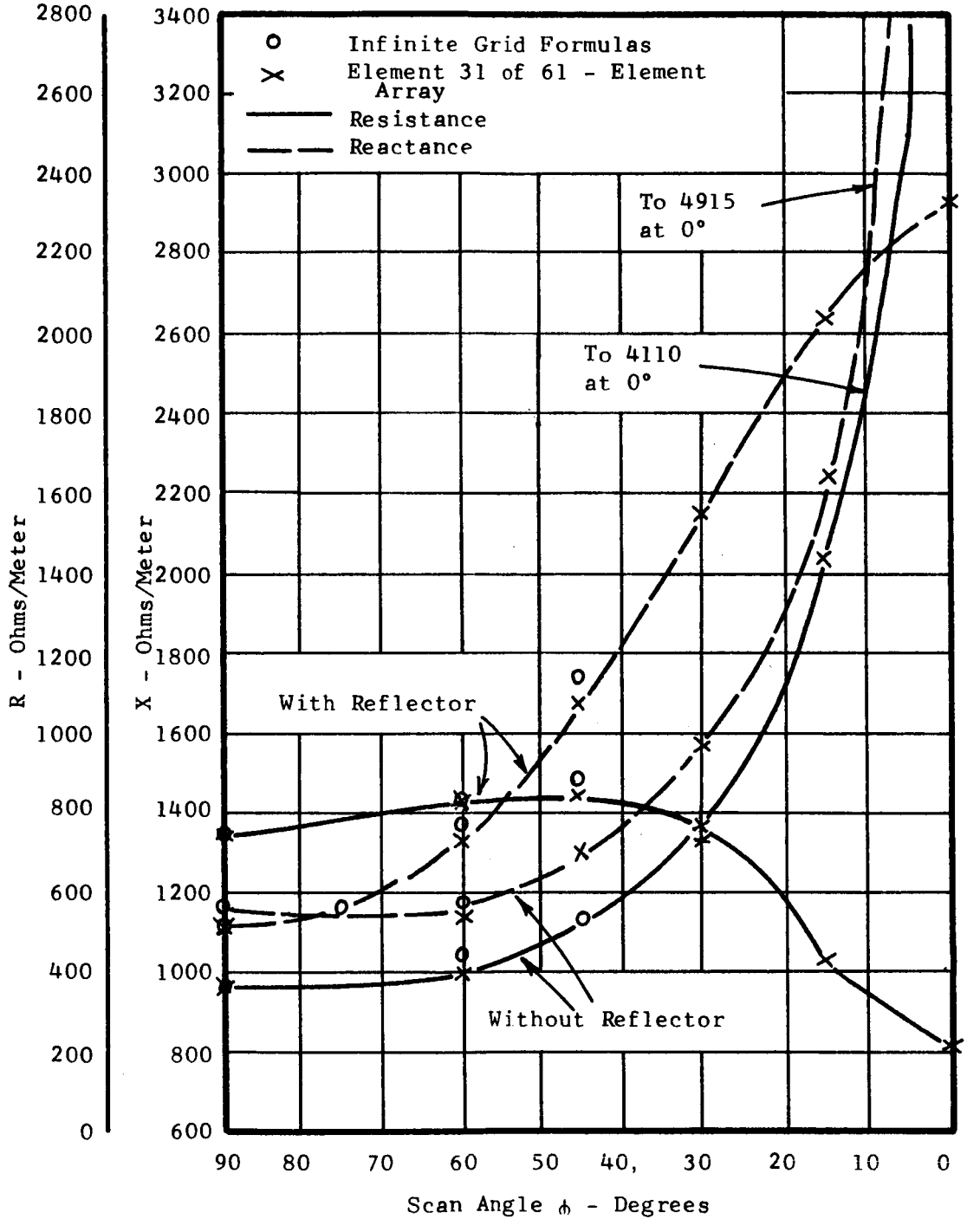

Fig. 9. Driving-Point Impedance vs Scan Angle of Infinite Wire Array (Element 31) and Infinite Grid

Allen[11] has carried out a computational program for 5 x 5 and 7 x 9 arrays of halfwave dipoles backed by a reflector and fed by generators of finite impedance. Each element was assumed to be fed independently by a generator whose impedance was the conjugate of the impedance of the center element of the array. Equal currents were assumed in all elements so that the array would approximate a section of an infinite array. This would of course require different source voltages since the driving-point impedance of all elements was not the same. Clearly, only the center elements were properly impedance-matched, although all elements would have been if this finite array had truly been a section of an infinite array.

Allen found the input impedance to the center element of his array as a function of distance S of the dipoles above a ground plane and element separation for a square-grid array (b = d in Fig. 4). This impedance varied considerably, indicating that input impedance is sensitive to variations in ground-plane distance and element separation.

He also computed the angles θ and ϕ, for a scanned beam, at which the radiation drops 3 db from its value at broadside. This is shown in Figs. 10 and 11 as the angle measured from the broadside direction in the E-plane for an E-plane scan and in the H-plane for an H-plane scan. These curves indicate that proper choices of element spacing and reflector distance are necessary to achieve wide scan angles. For example the poor choice of S = 0.375 λ and d = 0.8 λ would allow a scan angle of less than 20° from the vertical in the H-plane before the radiated power dropped 3 db. Normally d = 0.8 λ would not be chosen anyway because of the formation of grating lobes at large scan angles. In fact, Allen points that for spacing greater than $\lambda/2$ the angle corresponding

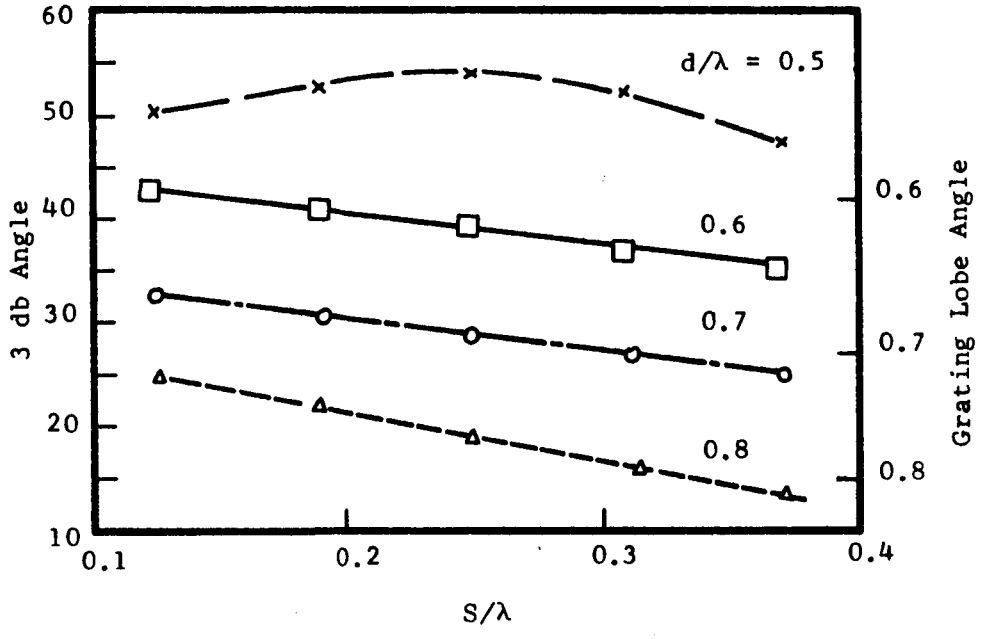

Fig. 10. Half-Power H-Plane Width of Gain Function

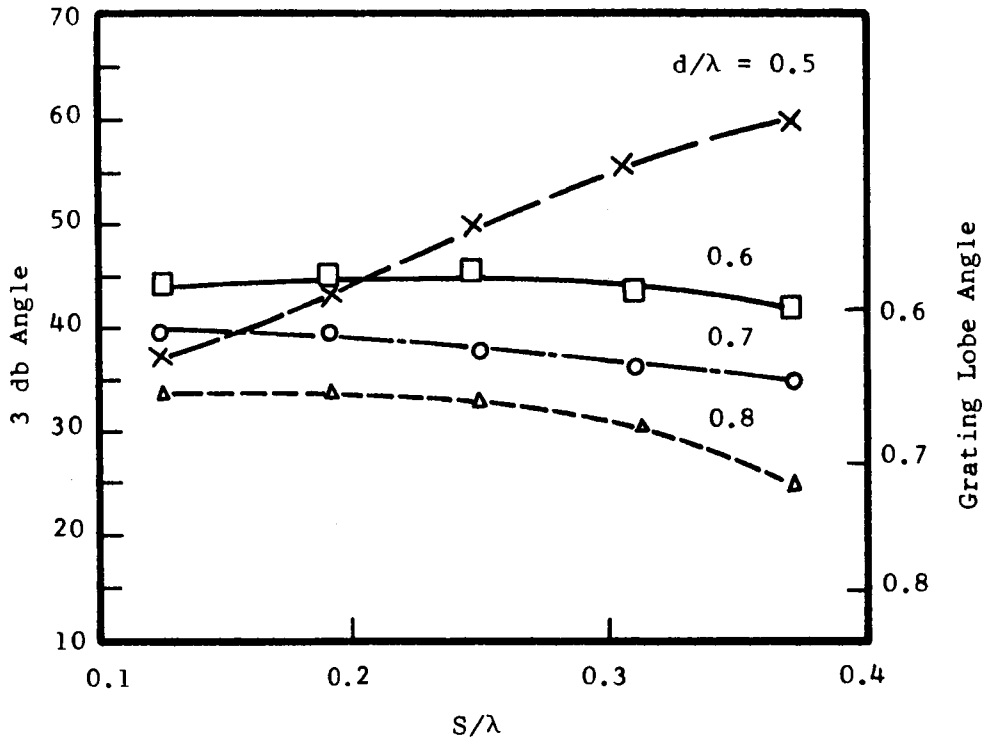

Fig. 11. Half-Power E-Plane Width of Gain Function

to the 3 db drop in power roughly corresponds to the angle over which an array can be scanned without grating lobe formation, given by

$$\frac{d}{\lambda} = \frac{1}{1 + \sin |\alpha_{max}|} \tag{13}$$

Kurtz[12] has carried out an experimental study of the self- and mutual impedances of dipole arrays. He tabulates these measured values for 1 x 10 and 5 x 10 arrays. His tables can be used for any generator impedances and any desired current taper over the array.

Mutual Coupling of Slots

Early important work on the theory of slots in waveguides was done by Stevenson.[13] He computed slot admittances and indicated an extension to arrays of slots. Kay and Simmons[14] have extended Stevenson's method to consider pairs of slots in a waveguide with mutual coupling. The procedures of Stevenson and of Kay and Simmons are quite complex and require extensive computer programs, so that only some of their more interesting results are given here. Kay and Simmons have calculated a dimensionless mutual coupling coefficient $\sum_o$ relating voltages across pairs of slots. Using the configuration of Fig. 12 and half wave slots this coefficient is shown in Fig. 13. In actuality this is only the portion of $\sum_o$ due to external coupling. For slots in a waveguide internal coupling is just as important as external. Kay and Simmons give an internal coupling coefficient which is of the same order of magnitude as the external coefficient, but this is not repeated here. It may be seen from Fig 13 that the coupling decreases with increasing slot separation, as might be expected.

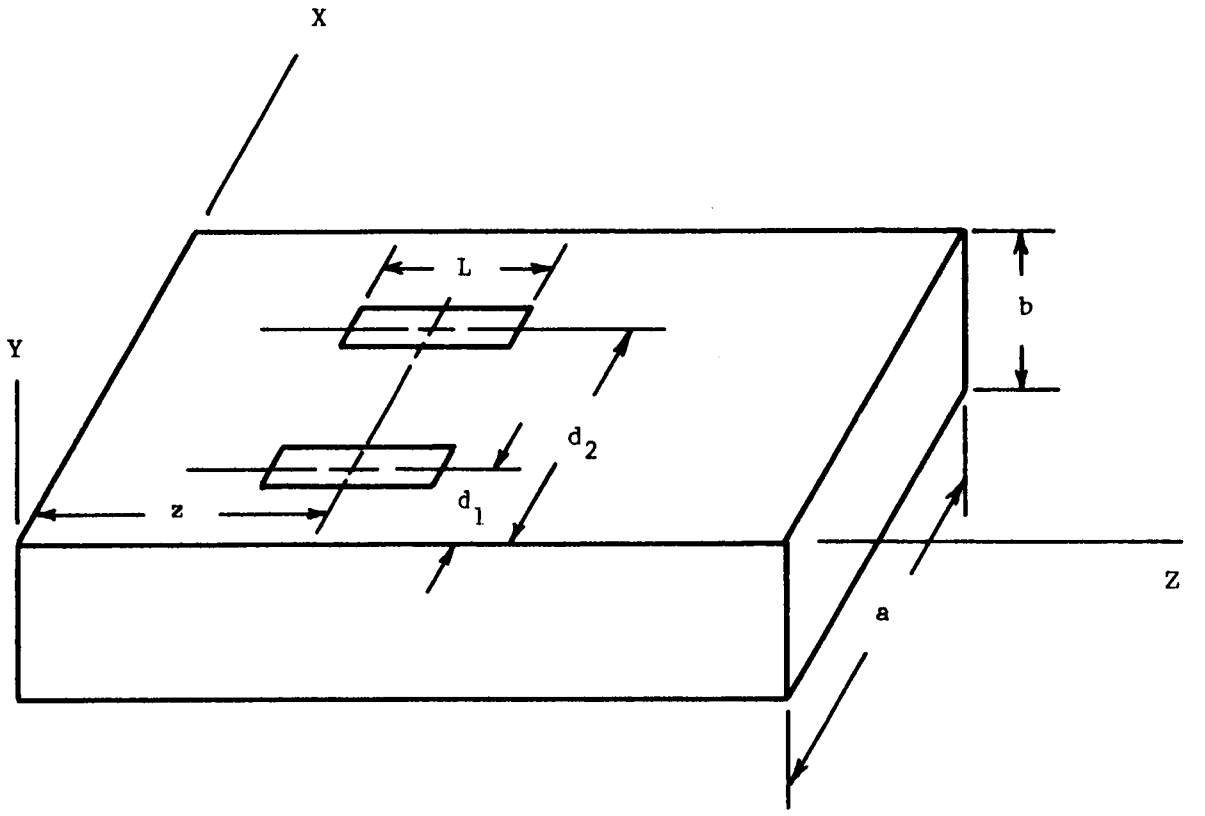

Fig. 12. Slot Parameters

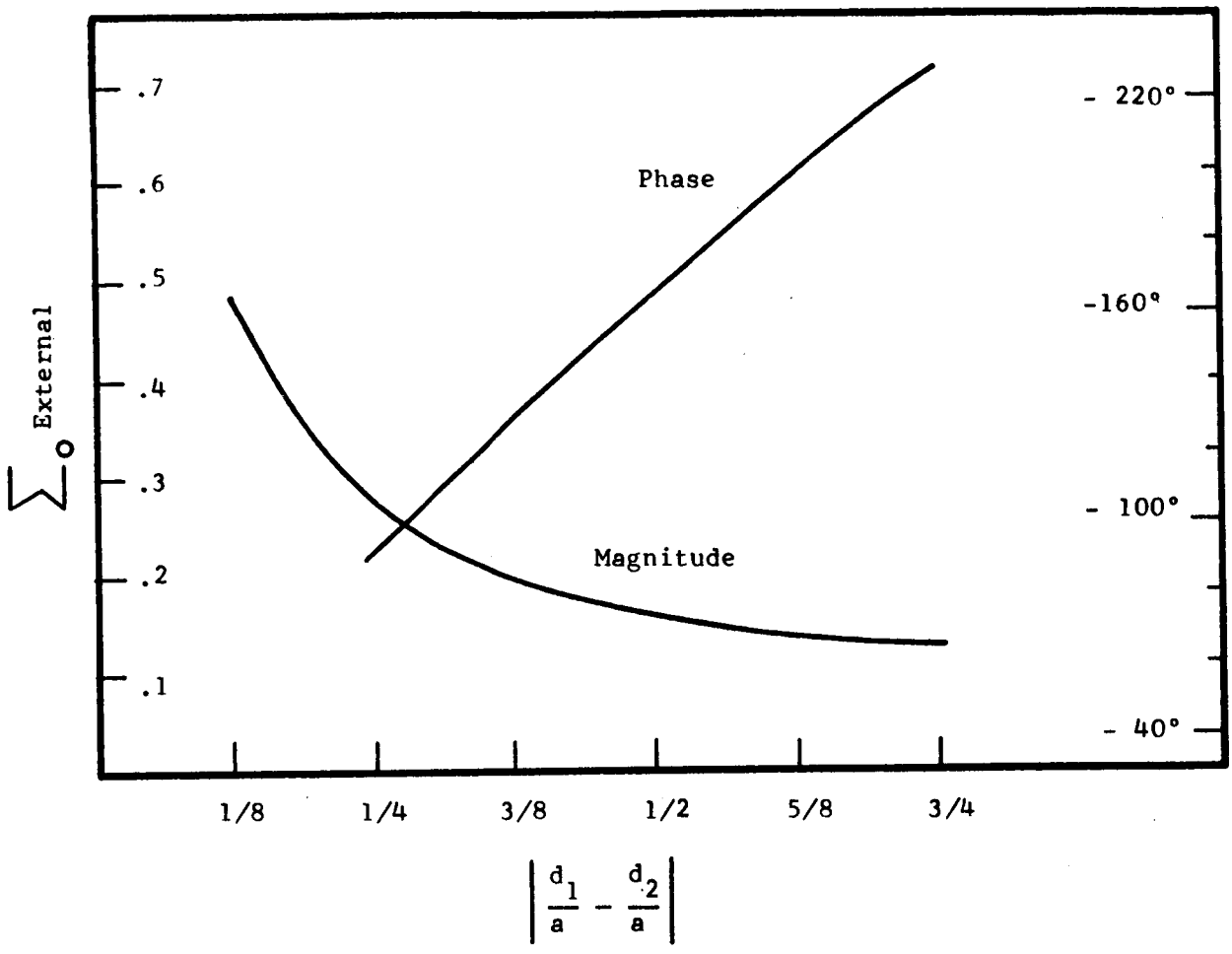

Fig. 13. Mutual Coupling Coefficient $\sum_o$

Figures 14 and 15 show radiation patterns from two slots showing the effects of mutual coupling. It is obvious that mutual coupling is highly important in determining the shape of the pattern. In these figures it is to be remembered that internal coupling plays an important part, and if it were eliminated (by separate waveguide feeds) the effect of mutual coupling on the pattern would probably be reduced. It appears again from these patterns that mutual coupling effects are greater for slots which are closer together.

Periodic Treatment of Arrays

A highly interesting treatment of an infinite slot array is given by Edelberg and Oliner.[15] They treat the radiation half space of an infinite array as being composed of waveguide cells as shown in Fig. 16. Each slot is fed from beneath the ground plane by a waveguide with dimensions a and b. For broadside radiation the walls of the "guide" in free space adjacent to the long slot dimensions are electric walls on which the tangential E field is zero, and the remaining walls are magnetic walls on which tangential H is zero. For a scan off broadside the free space "waveguides" maintain their shape but the character of the walls changes. With this treatment mutual impedances do not appear explicitly but are automatically taken into account in finding driving-point impedances.

The dominant propagating mode at broadside is a TEM mode (Note that this mode does not exist for a physical waveguide composed of conductors). When the array is scanned off broadside the dominant mode is no longer TEM but becomes a TE or a TM mode for scans in the H or E planes and a mixed mode for arbitrary scans.

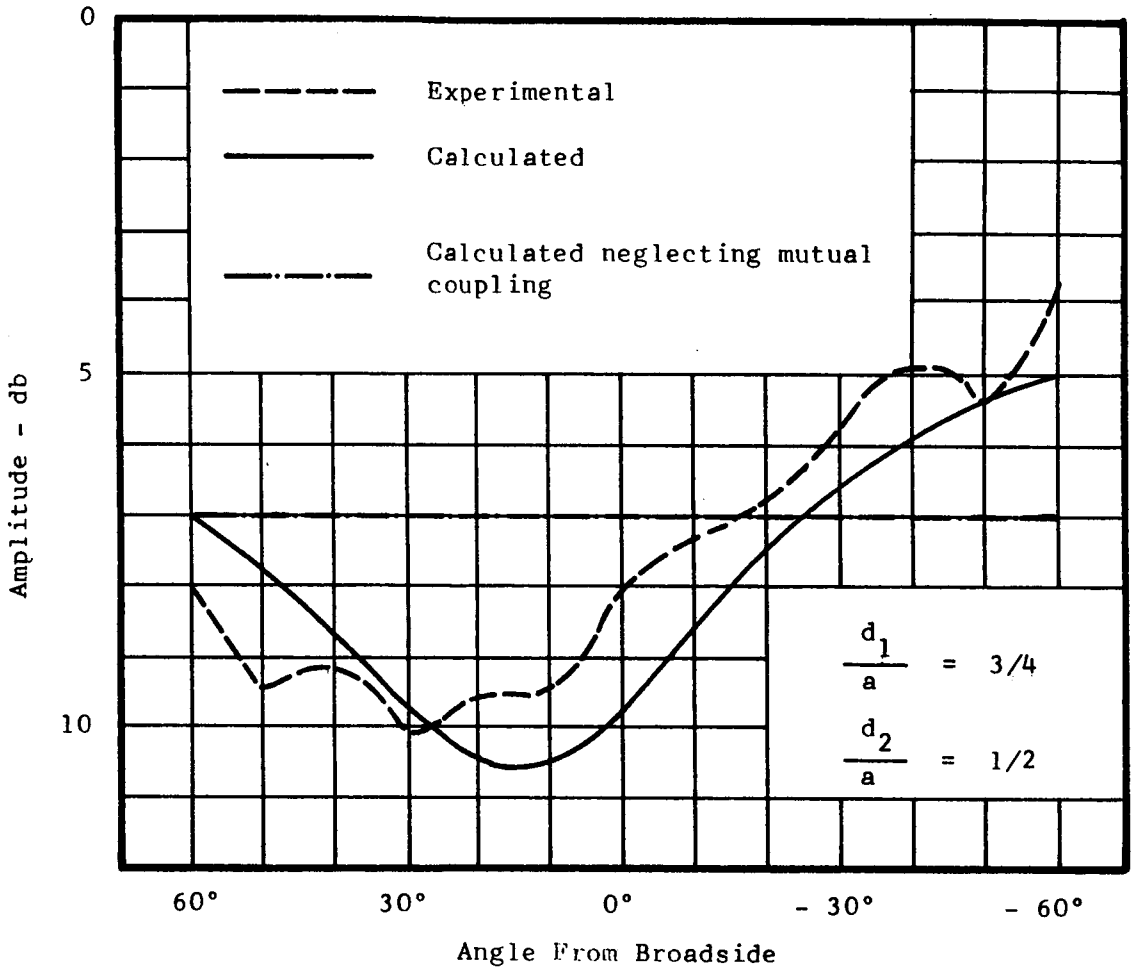

Fig. 14. Measured Reflection Coefficients for Resonant Slot Pairs

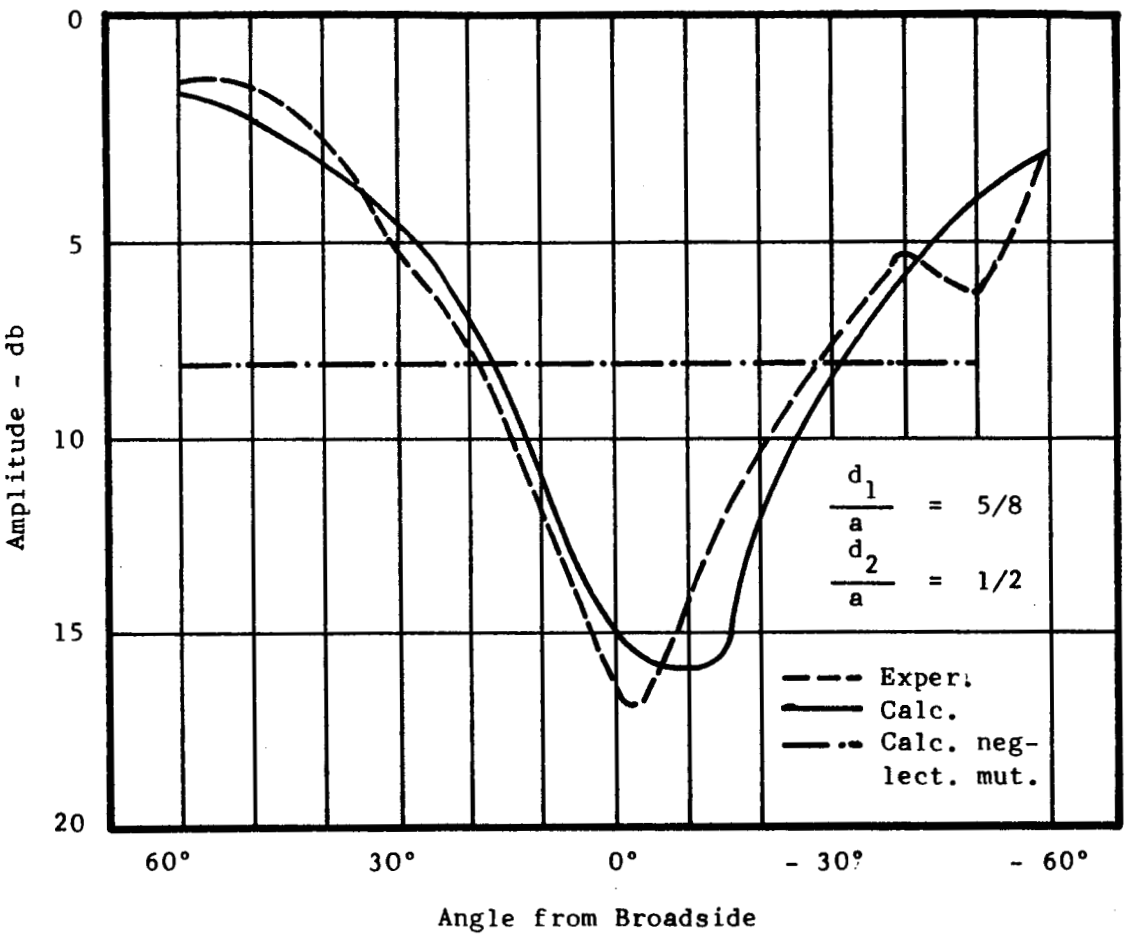

Fig. 15. Measured Reflection Coefficients for Resonant Slot Pairs

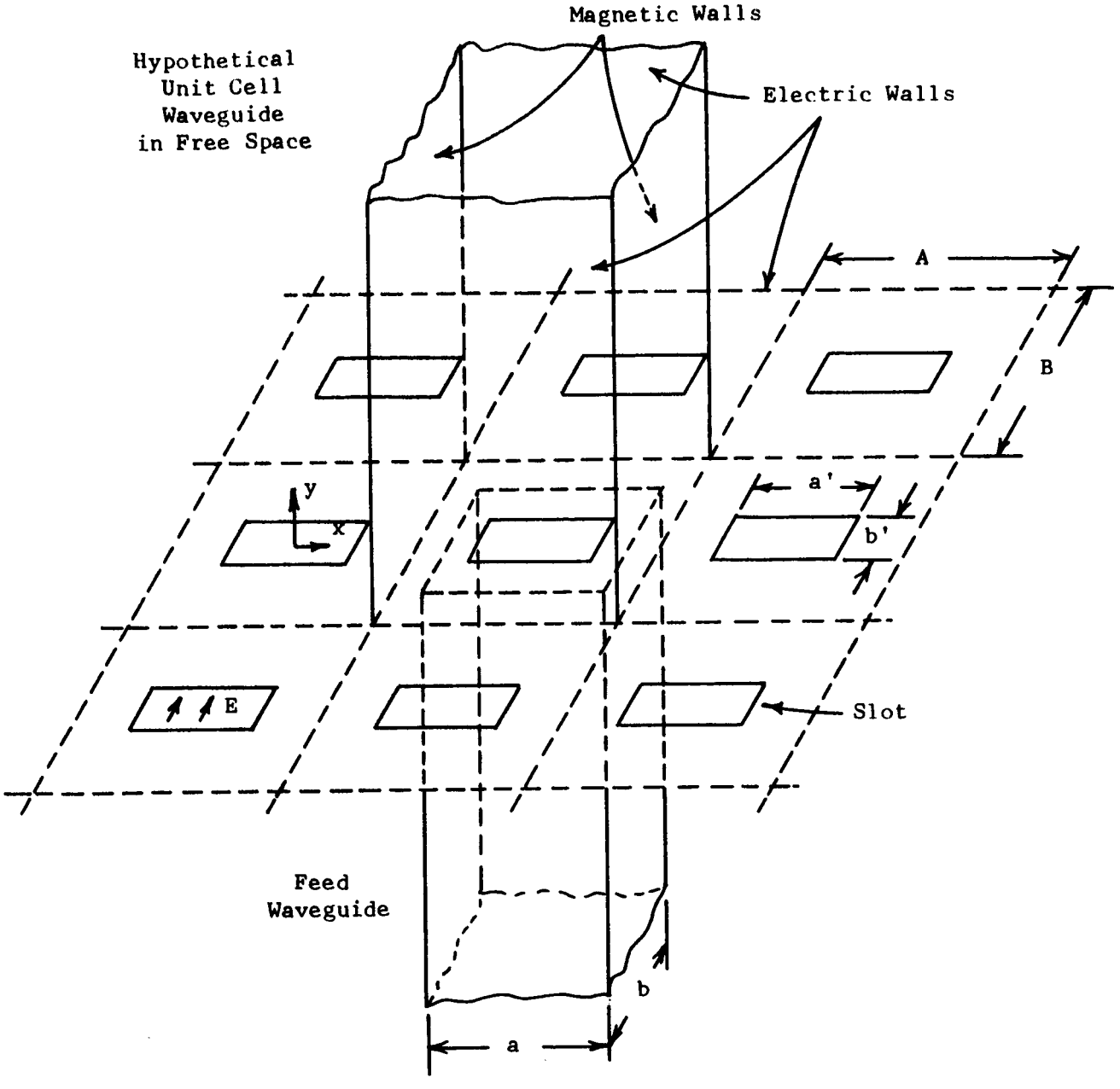

Fig. 16. Slot Array with Hypothetical Unit Cell

The procedure used is relatively straightforward and leads to results for driving-point admittances which can be easily calculated. Some of the resulting equations are given here, normalized to Y, the admittance of the feed waveguide.

For a single slot radiating into half space the conductance is

$$\left(\frac{G}{Y}\right)_{hs} = \frac{2\pi}{3}\ \frac{\lambda g}{\lambda}\ \frac{ab}{\lambda^2}\left[\frac{1-(a'/a)^2}{\cos(\pi\, a'/2a)}\right]^2\left[1-0.374\left(\frac{a'}{\lambda}\right)^2+0.130\left(\frac{a'}{\lambda}\right)^4\right] \tag{14}$$

For the same slot in an infinite array, with broadside radiation and only dominant mode propagation

$$\left(\frac{G}{Y}\right)_p = \frac{\lambda g}{\lambda}\ \frac{ab}{2AB}\left[\frac{1-(a'/a)^2}{\cos(\pi\, a'/2a)}\right]^2 \tag{15}$$

Approximately, for slots near resonance

$$\frac{(G/Y)_p}{(G/Y)_{hs}} \approx \frac{(\lambda/2)^2}{AB} \tag{16}$$

For practical array dimensions the feed waveguides might be packed as closely as possible. Then the ratio (16) becomes

$$\frac{(G/Y)_p}{(G/Y)_{hs}} \approx 1 \tag{17}$$

showing that for such an array operated at broadside, the conductance of a slot in the array differs little from that of the isolated slot.

If the electric wall spacing B is maintained less than λ but magnetic wall spacing A is made greater than λ higher order modes can propagate in the "waveguides" in space. Edelberg and Oliner point out in an interesting comment that the appearance of higher order modes corresponds to the appearance of grating lobes in the pattern.

If N of these higher order TE modes propagate, the conductance at broadside becomes

$$\frac{(G/Y)_p}{(G/Y)_{hs}} = \frac{3}{\pi}\frac{(\lambda/2)^2}{AB}\;\frac{1 + 2\sum_{n=1}^{N}\sqrt{1-(n\lambda/A)^2}\left[\frac{\cos n\pi a'/A}{1-(2na'/A)^2}\right]^2}{1 - 0.374(a'/\lambda)^2 + 0.130(a'/\lambda)^4} \qquad (18)$$

In the same way, if A is less than λ but B is greater than λ higher order TM modes propagate and the broadside conductance is

$$\frac{(G/Y)_p}{(G/Y)_{hs}} = \frac{3}{\pi}\frac{(\lambda/2)^2}{AB}\;\frac{1 + \sum_{n=1}^{N}\frac{2}{\sqrt{1-(n\lambda/B)^2}}\left[\frac{\sin(n\pi b'/B)}{n\pi b'/B}\right]^2}{1 - 0.374(a'/\lambda)^2 + 0.130(a'/\lambda)^4} \qquad (19)$$

Of greater interest than the broadside conductance is that for scan angles θ (colatitude angle measured from the z-axis) and ϕ (azimuth angle measured from the x-axis). For dominant mode propagation only this is

$$(G/Y)_{\theta,\phi} = (G/Y)_{\theta=0}\left[\frac{\cos\frac{\pi a'}{\lambda}\sin\theta\cos\phi}{1-\frac{2a'}{\lambda}\sin\theta\cos\phi}\right]^2 \cdot$$

$$\left[\frac{\sin\frac{\pi b'}{\lambda}\sin\theta\cos\phi}{\frac{\pi b'}{\lambda}\sin\theta\cos\phi}\right]^2\left[\frac{1-\sin^2\theta\cos^2\phi}{\cos\theta}\right] \qquad (20)$$

which can be reduced to simpler forms for E- and H-plane scanning.

Edelberg and Oliner also derive equations for slot susceptance. Their work here is of interest in that they point out that an isolated slot designed for resonance will no longer have zero susceptance when placed in an array. They then suggest that if the slots are designed for resonance at broadside in the array the susceptance value will change

little with scanning, particularly in the H-plane. Their equations for susceptance are not given here since they are for broadside only and do not show changes with scan angle.

Edelberg and Oliner[16] use the periodic waveguide approach also to find impedances for an infinite array of halfwave dipoles above a ground plane spaced at $\lambda/4$. Results are shown in Figs. 17 through 20 giving variation of driving-point impedance and VSWR as a function of scan angle. In determining VSWR the dipoles were deliberately designed to have a negative reactance of 0.3 Z_o (where Z_o is the impedance of the feed line) at broadside so that maximum reactance variation with scan angle is kept small. In Fig. 19 this design is not used; the reactance at broadside is zero.

Edelberg and Oliner give the relatively simple equations from which these figures were calculated, but these are not repeated since the results are shown graphically.

The baffles used by these authors and shown on the figures will be discussed in a later section.

Figure 17 indicates that driving-point resistance variation with scan angle is less for an H-plane scan with reflecting ground plane than it is for the other three conditions shown. Edelberg and Oliner do not give the variation of reactance with an E-plane scan for comparison purposes, but Fig. 20 does give the VSWR for each dipole as a function of scan angle for E- and H-plane scans. Figs. 17 and 20 taken together indicate that driving-point resistance and VSWR remain more uniform with scan angle for the H-plane than for the E-plane, and this would then be the preferred scanning plane if a scan in only one plane is desired.

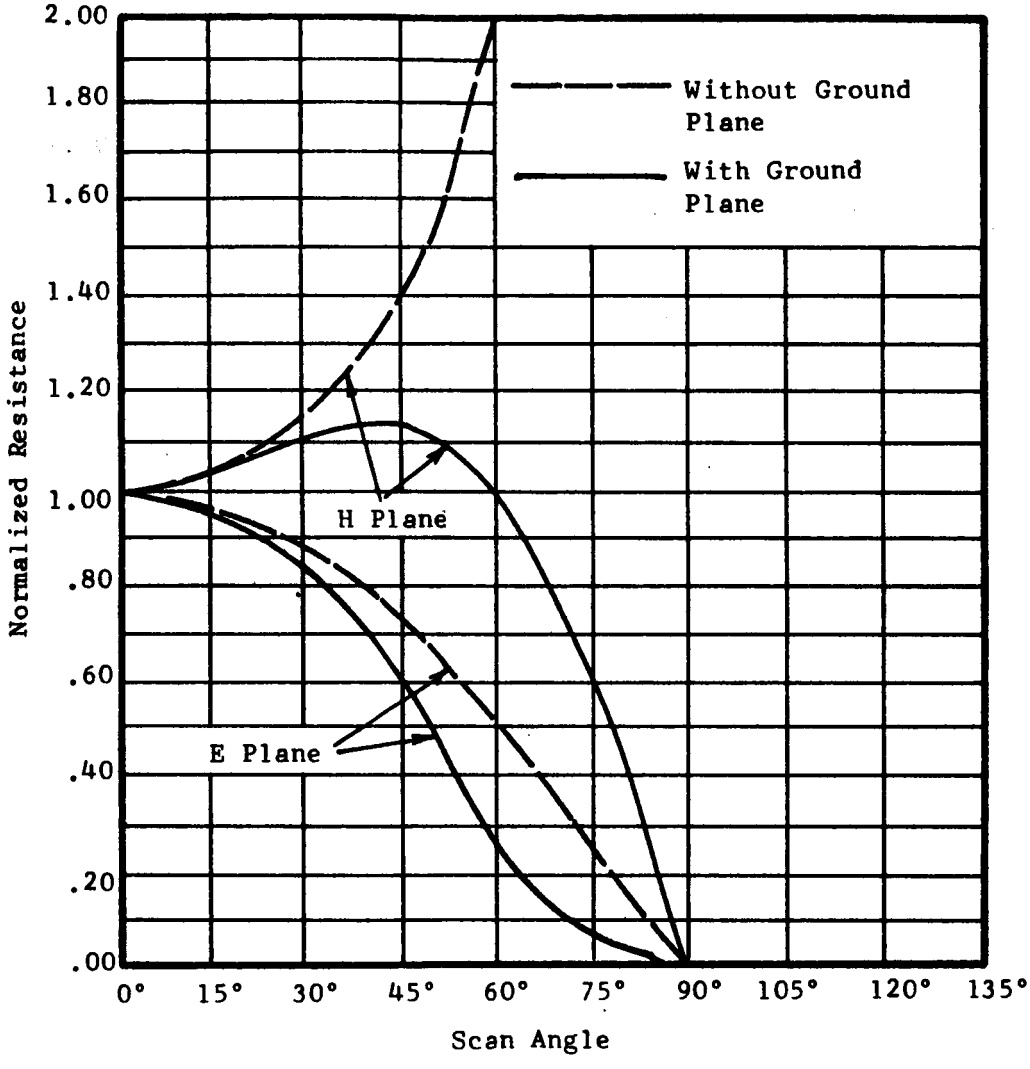

Fig. 17. Input Resistance of Dipole Array with and without Ground Plane

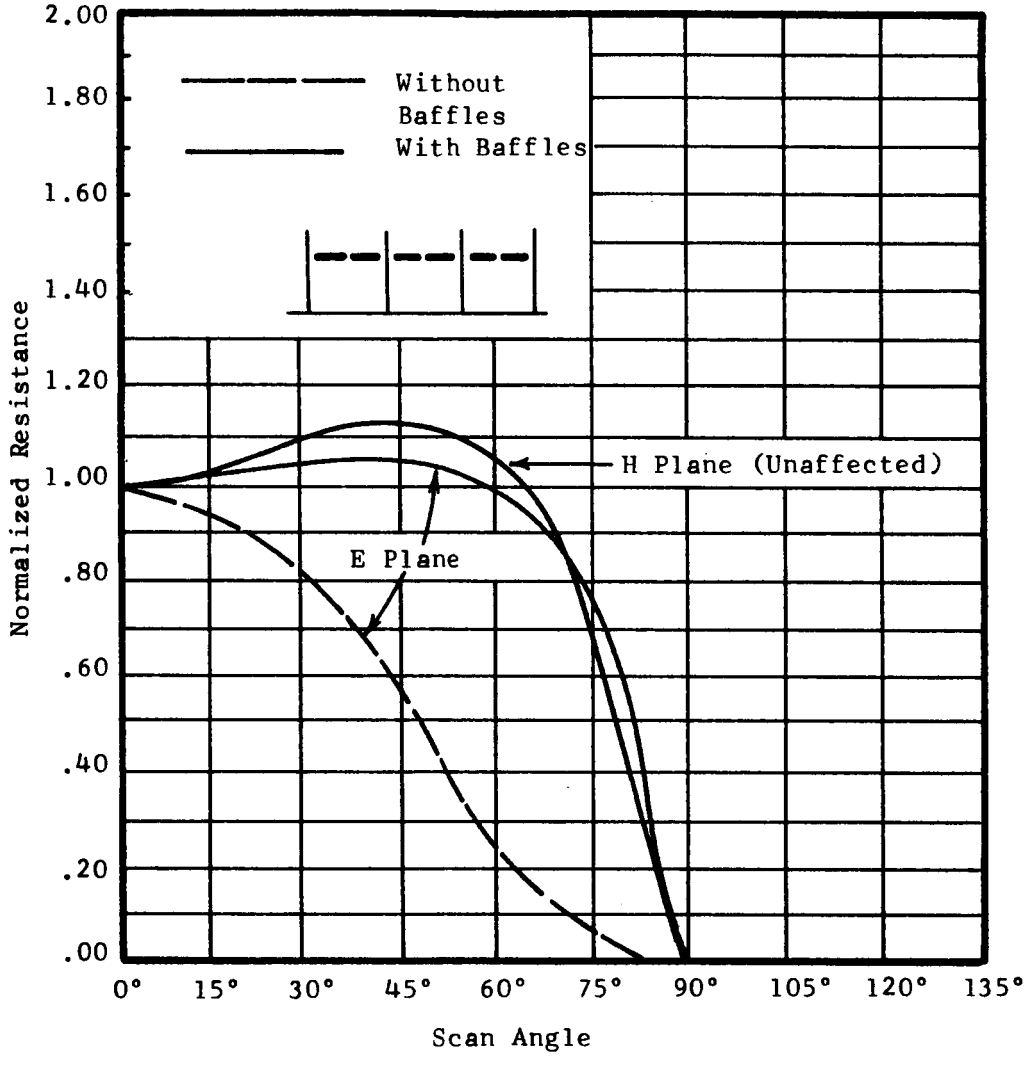

Fig. 18. Effects of Compensating Baffles on Input Resistance of Dipole Array

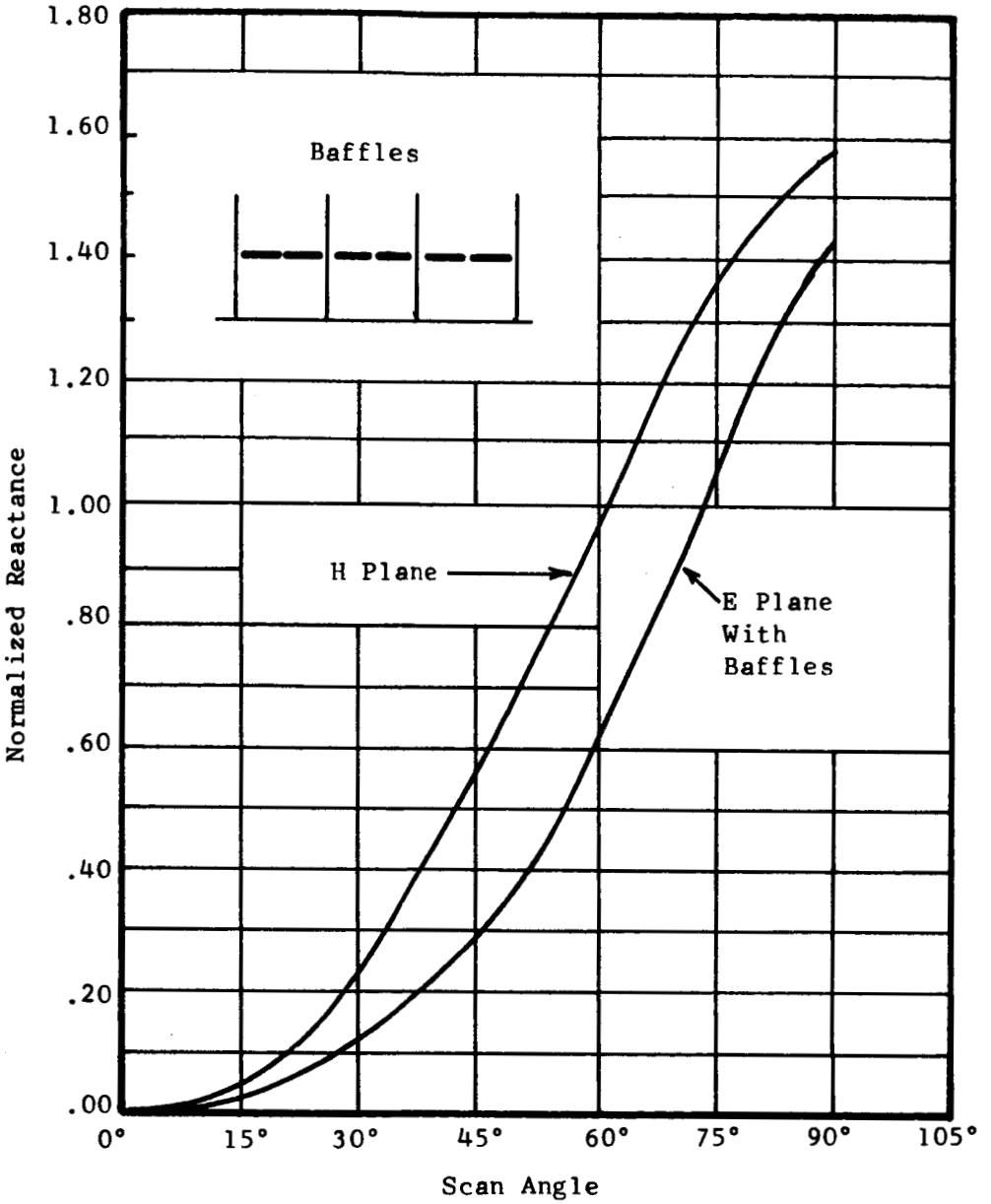

Fig. 19. Input Reactance of Dipole Array

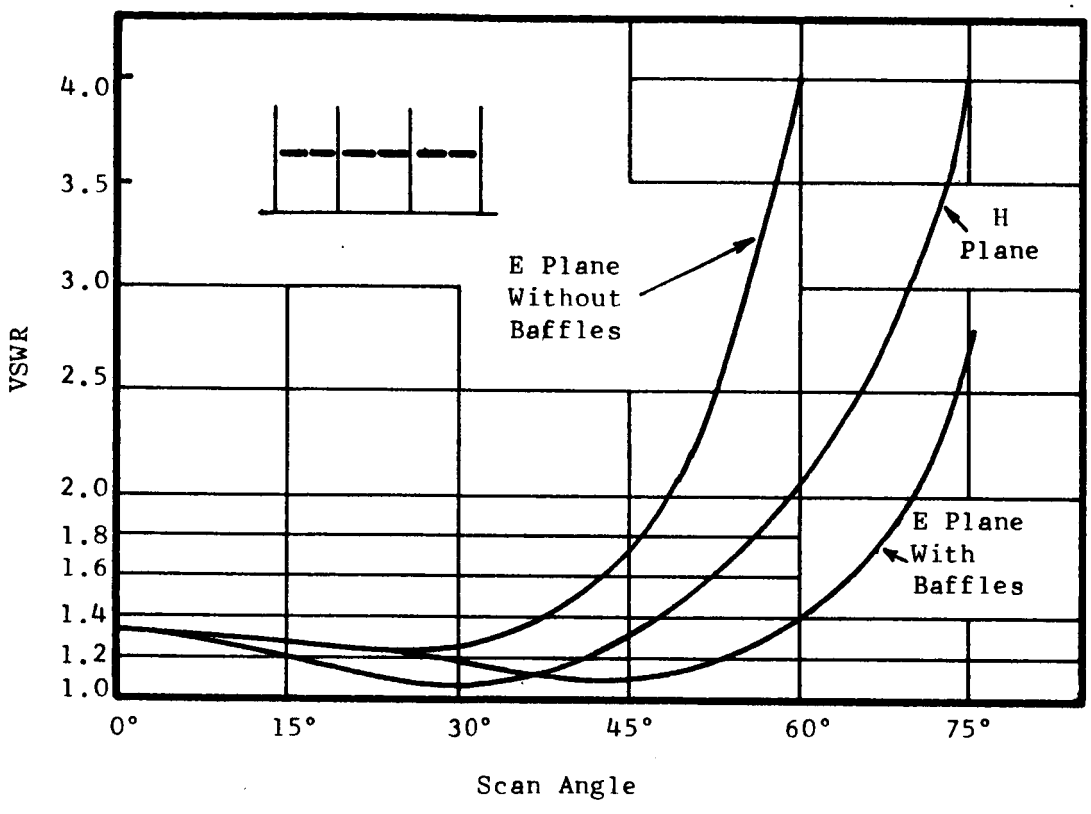

Fig. 20. Effects of Compensating Baffles on VSWR of Dipole Array

Helical array elements have been studied by Stratioti and Wilkinson.[17] They point out that the mutual coupling between two helices is less than between parallel dipoles. A problem is using helical elements which they do not seem to have considered will be mentioned in a later section.

III. METHODS OF COMPENSATION

Proper Design of Array

An appropriate element choice is the first consideration, but other factors generally make it desirable to use dipoles above a ground plane or slots.

Element shape is a factor. Edelberg and Oliner[16] designed dipole elements to have a negative reactance at broadside in the array. Then, as reactance increased with scan angle, the greatest magnitude of reactance remained smaller than would have been the case if zero reactance at broadside had been used.

Element spacing must be considered. As a first thought one would space the elements as widely as possible, since mutual coupling between a pair of elements decreases with distance. However, the results of Allen[11] given in Figs. 10 and 11 indicate that for dipoles above a ground plane with rows and columns equally spaced the scan angle at which power drops 3 db from broadside is greater for smaller spacings. Thus smaller spacings give a greater scan angle, at least in the range of spacings (0.5λ to 0.8λ) considered. The angle of scan at which power drops 3 db is relatively insensitive to ground-plane distance in the range shown (except for element spacing of $\lambda/2$).

For scanning in one plane one should use the plane in which power loss with scan angle is smallest. Thus for dipoles above a ground plane the work of Edelberg and Oliner indicate that the H-plane is the proper choice.

It is obvious that the system should be designed if possible so that large scan angles are unnecessary.

If the impedance changes with scan angle cause generator instability they can be protected with circulators or isolators.

Little work has been done to verify the intuitive notion that mutual coupling effects will be more severe if all elements are fed by one source than would be true if they were fed independently. This seems likely, however, because of uncontrolled internal couplings within the array. For a non-independent feed system the use of isolators or circulators seems highly desirable.

External Compensation

Edelberg and Oliner describe an ingenious way of decreasing the driving-point impedance variation with scan angle for dipole elements.[16] For an array above a ground plane they add conducting baffles between the ends of the dipoles as shown in Fig. 18. The height of the baffles was chosen as the dipole height plus approximately $\lambda/2\pi$. As might be expected the baffles do not change the array behavior for an H-plane scan appreciably. For the E-plane scan, however, Fig. 18 shows the considerable improvement in driving-point resistance brought about by the addition of the baffles. The change of resistance with scan angle is now less than for the H-plane scan. Fig. 20 shows the great improvement in VSWR as a function of scan angle caused by the addition of the baffles.

The addition of conducting baffles to an array structure in an effort to lower mutual impedance between elements is a natural thought, and as can be seen effects a great improvement in impedance variation. However, apart from instability problems, the most important consideration for a scanned array is radiated power in a particular scan direction. Edelberg and Oliner unfortunately do not consider this most important

question. It seems probably that the addition of baffles merely makes each element more directive. Then the addition of baffles does not solve the major problem, and it seems likely that radiated power in a particular scan direction will not increase when baffles are added. The source of trouble is simply changed from impedance mismatch to a problem of too-great element directivity. Ideally, one would like to have elements with negligibly small coupling by means of the near fields without sacrificing the omnidirectional properties of the radiation field of the element, but it is by no means certain that such an element can be found.

This problem of course exists with the use of other types of elements, such as the helices discussed previously.[17] A decrease of mutual impedance by a change to another type of element is not a solution to the problems which arise.

Compensation by Connecting Circuits

A compensation scheme of potentially great utility has been proposed by Hannan.[18] He and his co-workers match the driving-point impedances of the array elements (which change with scan angle) by means of lossless circuits connecting the element feed lines. This introduces a susceptance in each feed line which also changes with scan angle. Thus at least partial compensation of impedance variation can be provided.

The matching network for a part of the array is shown in Fig. 21 (a) and an equivalent network in Fig. 21 (b) which gives a susceptance for each feed line which varies with generator phasing. In the actual network

$$I_u + I_d = jB(V_\alpha - V_{2\alpha}) + jB(V_\alpha - V_o) \qquad (21)$$

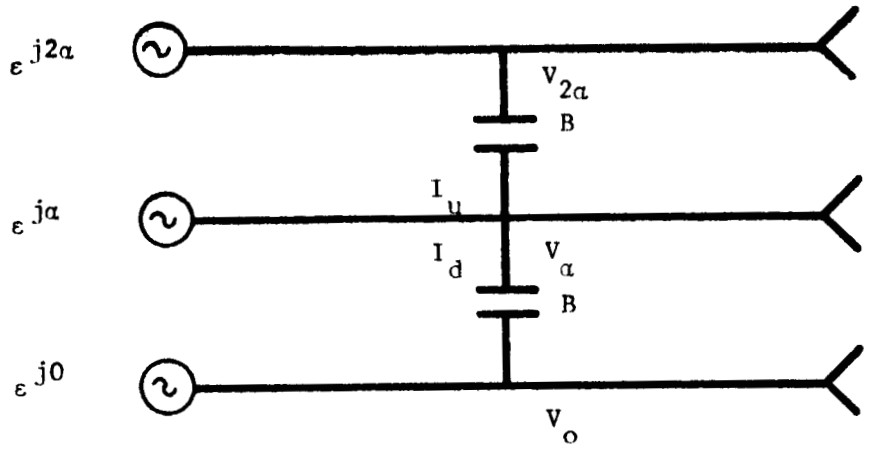

(a)

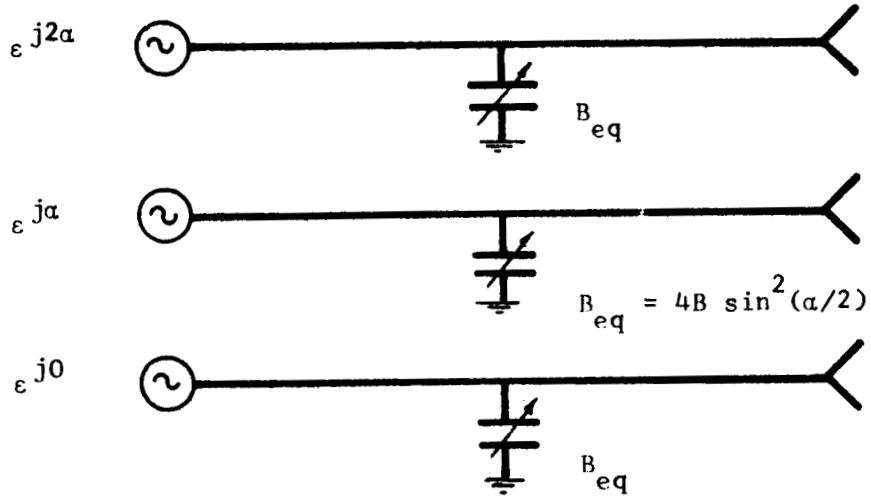

(b)

Fig. 21. Derivation of Equivalent Circuits for Infinite Linear Array

The equivalent admittance for the center feed line is

$$Y_{eq} = \frac{I_u + I_d}{V_\alpha} = jB\left(2 - \frac{V_{2\alpha}}{V_\alpha} - \frac{V_o}{V_\alpha}\right) \tag{22}$$

But with constant phase differences for the applied voltage and equal voltage amplitudes

$$\frac{V_{2\alpha}}{V_\alpha} = \frac{V_\alpha}{V_o} = \varepsilon^{j\alpha} \tag{23}$$

Substitution of (23) into (22) yields

$$Y_{eq} = j\,4\,B\,\sin^2\left(\frac{\alpha}{2}\right) = j\,B_{eq} \tag{24}$$

Thus it is seen that the connecting circuits introduce an equivalent susceptance into each feed line which varies with generator phasing. It could not of course be expected that this variable susceptance plus any fixed susceptance in the feed line would vary in a manner that would allow it to cancel exactly the changes in antenna susceptance with generator phasing, but one would certainly feel by proper choice of magnitude and sign (inductive or capacitive) of B that antenna impedance changes with scan angle could be compensated to some degree. This belief is shown by Hannan to be justified.

Hannan describes the compensation procedure quantitatively for a planar array of dipoles whose impedance as a function of scan angle was calculated by Allen.[11,19] Capacitors were placed between adjacent feed lines for elements in the E-plane of the array and inductors between feed lines of elements in the H-plane. Fortunately E-plane compensation does not affect the H-plane scan, and vice versa. In addition compensation is made much simpler by the fact that addition of the compensating

elements does not change the impedance at broadside, from Eq. (24) giving $B_{eq} = 0$ at $\alpha = 0$.

The matching process used by Hannan is not entirely straightforward. He does not for example give an explicit equation for finding the capacitive susceptances ($B_E = +0.27$, normalized to feed line) connecting the E-plane feed lines and the inductive susceptances ($B_H = -0.26$) connecting the H-plane lines. This would become straightforward if it were desired to match only for E-plane and H-plane scans, but Hannan matches also for a diagonal (D) scan.

The matching network (showing equivalent susceptances as given by Eq. 24 for the connecting elements) and the impedances resulting from each matching step are given in Fig. 22. The matching network adjacent to the balun is for the purpose of centering the impedances for the various scan directions on the reflection chart. (Alternatively it could be used to give zero VSWR at a scan angle of 0°.)

Hannan desired in this matching to minimize the VSWR for scan angles of 60° in E-, H-, and D-planes, or roughly in a cone of 120°.

VSWR after the first matching network is added is 14 db for 60° scan in both E- and H-planes, Fig. 22(b). The addition of L_a merely rotates the impedances so that they are placed in a favorable position for the addition of admittance B_{eqE}. (Note that Hannan's chart is reversed from some Smith chart forms). In Fig. 22(d), B_{eqE} has been added. This has value for a 60° scan angle of

$$4 B_E \sin^2\left(\frac{\alpha}{2}\right) = 4 (0.27) \sin^2(30°) = 0.27 \qquad (27)$$

Note that it does not affect the H-plane impedance.

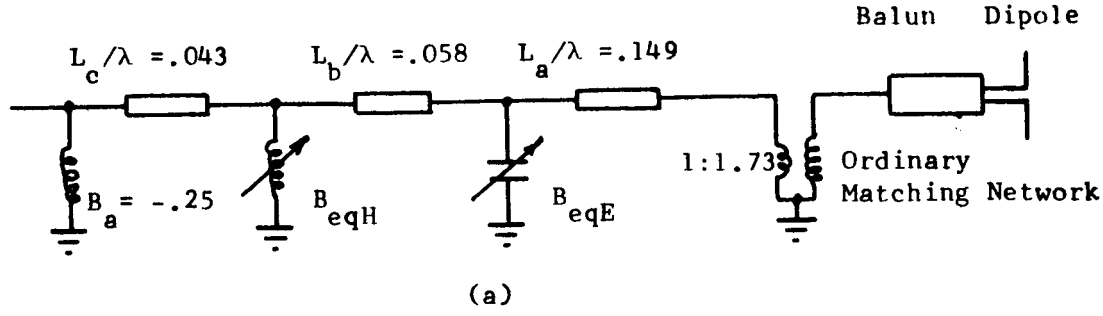

(a)

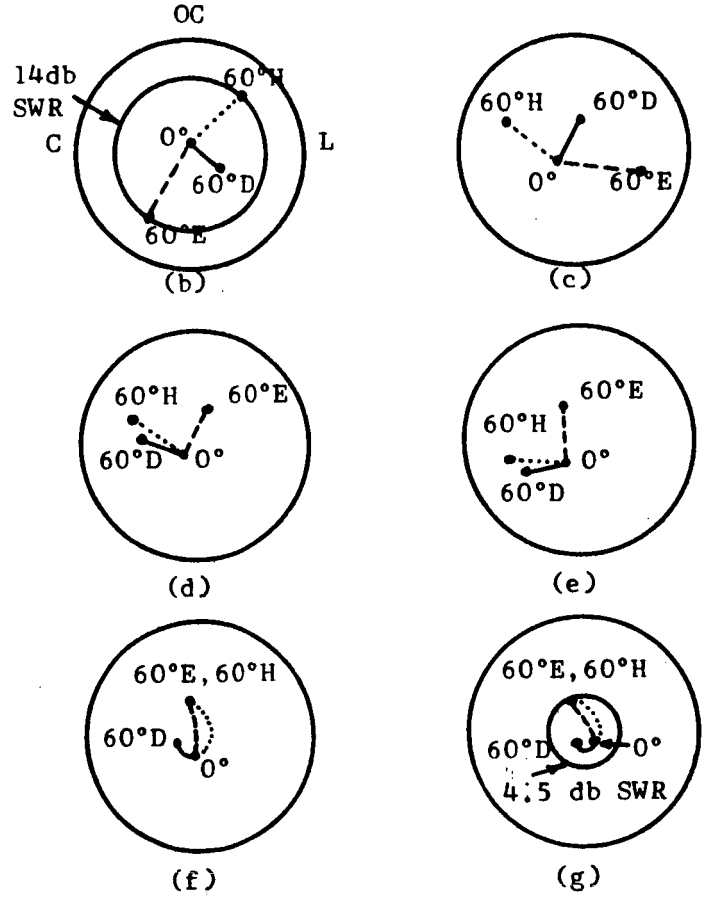

Fig. 22. Matching Networks and Results of Impedance Matching

The impedance loci are again rotated by a length of line, L_b, and B_{eqH} is added giving the impedances shown in Fig. 22(e). Finally L_c and a fixed susceptance B_a are added to center the three impedance loci on the chart. The final result is given by Fig. 22(g).

With only the matching given by the series reactance and transformer adjacent to the dipole, VSWR for E- and H-plane scans of 60° is 14 db, giving a power loss due to reflections of 2.6 db. After complete matching the corresponding VSWR and reflection loss are 4.5 db and 0.3 db.

Since no changes are made external to the array the decreased reflection loss appears entirely in radiated power in the desired scan direction. This differs from the procedure of improving VSWR by placing baffles around the array elements for which it was pointed out previously that the VSWR improvement might not result in increased power in the scan direction because of changed directional properties of each antenna element.

Hannan points out that the connecting susceptances can be realized in many ways, by lumped elements as indicated for this unbalanced line feed, by lengths of line between the feed lines, or by slots between adjacent waveguides in a closely packed waveguide feed system. Implementation in a strip transmission line feed also seems quite feasible.

Hannan considers matching at one frequency only. It is probable that the addition of the matching circuitry will narrow the frequency bandwidth of the system. Matching for both a wide scan angle and over a wide bandwidth is in all likelihood an extremely difficult problem.

This impedance-matching method requires a knowledge of the input impedance of each element, prior to the matching, at broadside and as a function of scan angle (often a knowledge at the maximum desired scan

angle would be sufficient). If this impedance cannot be calculated with sufficient accuracy before the array is constructed, it must be measured. Then the technique becomes essentially corrective in nature and thus more difficult to apply to an already-constructed system.

In either case, however, it appears to offer perhaps the best method available for improving scanned-array performance.

IV. CONCLUSIONS

This study has shown that mutual coupling between elements of an array causes the input impedance of an element to differ from its value if it were isolated, makes the impedance of an element near the edge different from that of an interior element, and makes the impedance of all elements a function of the array scan angle. The impedance changes cause the element and generator to be mismatched at some scan angles and thus lend to a loss in radiated power. For arrays in which the contribution of elements near the edge is significant the different impedance for edge and center elements, and their different rate of change with scan angle, will alter the relative amplitudes and phases of the array currents from their calculated values assuming that they are fed by generators whose phases are varied to produce scanning. This gives distortion of the radiation patterns and causes errors in the beam-pointing direction.

Various methods of overcoming this problem are discussed in the report. Proper design of the array is the first factor. This requires attention to element type, size, and spacing. It may be desirable to design elements with a reactance at broadside opposite in sign to the change in reactance with scan angle. Equations and curves are given in this report from which reactance changes for some types of arrays can be found. Intuitively one would design arrays with wide element spacing to decrease mutual coupling effects, and this is probably the correct procedure for spacings up to $\lambda/2$, but it was shown in this report that an increase in spacing beyond that point will result in poorer scanning performance for some arrays.

External adjustments, such as placing baffles between array elements, may be made to improve VSWR changes with scan angle, but it is possible that this does not increase radiated power in a desired scan direction.

A method of internal coupling to compensate for the external coupling problem was discussed in this report. It appears to offer perhaps the best solution to the problem of mutual impedance effects on the performance of scanned arrays.

The published work dealing with the mutual impedance problem is not extensive. Mutual impedances between array elements have been calculated for only a very few types of elements, and even then not very extensively for different element sizes, spacings, etc. Major problems, such as the effect of external baffles on radiation (rather than VSWR), have not been studied. Wide frequency band compensation does not seem to have been considered by anyone. These are only a few of the problems remaining to be studied in this highly important area.

V. REFERENCES

1. Blasi, E. A. and R. S. Elliott, "Scanning antenna arrays of discrete elements," IRE Trans. on Antennas and Propagation, vol. AP-7, no. 4, pp. 435-436; October, 1959.

2. Carter, P. S., "Circuit relations in radiating systems and applications to antenna problems," Proc. of the IRE, vol. 20, no. 6, pp. 1004-1041; June, 1932.

3. Carson, J. R., "A generalization of the reciprocal theorem," Bell System Tech. J., vol. 3, pp. 393-399; July, 1924.

4. Carson, J. R., "Reciprocal theorems in radio communication," Proc. IRE, vol. 17, pp. 952-956; June, 1929.

5. Brown, R. G., et. al. "Lines, Waves, and Antennas," The Ronald Press Company, New York; 1961.

6. King, H. E., "Mutual impedance of unequal length antennas in echelon," IRE Transactions on Antennas and Propagation, vol. AP-5, No. 3, pp. 306-313; July, 1957.

7. Jordan, E. C., "Electromagnetic Waves and Radiating Systems," Prentice-Hall, Inc., Englewood Cliffs, New Jersey; 1950.

8. Jasik, H., ed., "Antenna Engineering Handbook," McGraw-Hill Book Company, New York; 1961.

9. Carter, P. S., Jr., "Mutual impedance effects in large beam scanning arrays," IRE Trans. on Antennas and Propagation, vol. AP-8, no. 3, pp. 276-285; May, 1960.

10. Stratton, J. A., "Electromagnetic Theory," McGraw-Hill Book Company, Inc., New York, pp. 349-361; 1941.

11. Allen, J. E., "Gain and impedance variation in scanned dipole arrays," IRE Trans. on Antennas and Propagation, vol. AP-10, no. 5, pp. 566-572; September, 1962.

12. Kurtz, L. A., et. al., "Mutual-coupling effects in scanning dipole arrays," IRE Trans. on Antennas and Propagation, vol. AP-9, no. 5, pp. 433-443; September, 1961.

13. Stevenson, A. F., "Theory of slots in rectangular waveguides," J. Appl. Phys., vol. 19, pp. 24-38; January, 1948.

14. Kay, A. F. and A. J. Simmons, "Mutual coupling of shunt slots," IRE Trans. on Antennas and Propagation, vol. AP-8, no. 4, pp. 389-400; July, 1960.

15. Edelberg, S. and A. A. Oliner, "Mutual coupling effects in large antenna arrays: part I - slot arrays," IRE Trans. on Antennas and Propagation, vol. AP-8, no. 3, pp. 286-297; May, 1960.

16. Edelberg, S. and A. A. Oliner, "Mutual coupling effects in large antenna arrays II: compensation effects," IRE Trans. on Antennas and Propagation, vol. AP-8, no. 4, pp. 360-367; July, 1960.

17. Stratioti, A. R. and E. J. Wilkinson, "An investigation of the complex mutual impedance between short helical array elements," IRE Trans. on Antennas and Propagation, vol. AP-7, no. 3, pp. 279-280; July, 1959.

18. Hannan, P. W., et. al., "Impedance matching a phased-array antenna over wide scan angles by connecting circuits," IEEE Trans. on Antennas and Propagation, vol. AP-13, no. 1; January, 1965.

19. Allen, J. L., et. al., "Phased Array Radar Studies, 1 July, 1960 to 1 July, 1961," Lincoln Laboratory, MIT, Lexington, Tech. Report 236; November, 1961.